Atmos. Chem. Phys., 8, 1763–1788, 2008
www.atmos-chem-phys.net/8/1763/2008/

Atmospheric Chemistry and Physics

Intercomparison of UV-visible measurements of ozone and NO_2 during the Canadian Arctic ACE validation campaigns: 2004–2006

A. Fraser[1], F. Goutail[2], K. Strong[1], P. F. Bernath[3,4], C. Boone[4], W. H. Daffer[5], J. R. Drummond[6,1], D. G. Dufour[7], T. E. Kerzenmacher[1], G. L. Manney[8,9], C. T. McElroy[10,1], C. Midwinter[1], C. A. McLinden[10], F. Nichitiu[1], C. R. Nowlan[1], J. Walker[1], K. A. Walker[1,4], H. Wu[1], and J. Zou[1]

[1]Department of Physics, University of Toronto, Toronto, Canada
[2]Service d'Aéronomie du Centre Nationale de la Recherche Scientifique, Verrières le Buisson, France
[3]Department of Chemistry, University of York, Heslington, UK
[4]Department of Chemistry, University of Waterloo, Waterloo, Canada
[5]Columbus Technologies and Services Inc., Pasadena, USA
[6]Department of Physics and Atmospheric Science, Dalhousie University, Halifax, Canada
[7]Picomole Instruments Inc., Edmonton, Canada
[8]Jet Propulsion Laboratory, California Institute of Technology, Pasadena, USA
[9]New Mexico Institute of Mining and Technology, Socorro, USA
[10]Environment Canada, Downsview, Ontario, Canada

Received: 25 October 2007 – Published in Atmos. Chem. Phys. Discuss.: 23 November 2007
Revised: 14 February 2008 – Accepted: 26 February 2008 – Published: 26 March 2008

Abstract. The first three Canadian Arctic ACE validation campaigns were held during polar sunrise at Eureka, Nunavut, Canada (80° N, 86° W) from 2004 to 2006 in support of validation of the ACE (Atmospheric Chemistry Experiment) satellite mission. Three or four zenith-sky viewing UV-visible spectrometers have taken part in each of the three campaigns. The differential slant column densities and vertical column densities of ozone and NO_2 from these instruments have been compared following the methods of the UV-visible Working Group of the NDACC (Network for Detection of Atmospheric Composition Change). The instruments are found to partially agree within the required accuracies for both species, although both the vertical and slant column densities are more scattered than required. This might be expected given the spatial and temporal variability of the Arctic stratosphere in spring. The vertical column densities are also compared to integrated total columns from ozonesondes and integrated partial columns from the ACE-FTS (ACE-Fourier Transform Spectrometer) and ACE-MAESTRO (ACE-Measurements of Aerosol Extinction in the Stratosphere and Troposphere Retrieved by Occultation) instruments on board ACE. For both species, the columns from the ground-based instruments and the ozonesondes are found to generally agree within their combined error bars. The ACE-FTS ozone partial columns and the ground-based total columns agree within 4.5%, averaged over the three campaigns. The ACE-MAESTRO ozone partial columns are generally smaller than those of the ground-based instruments, by an average of 9.9%, and are smaller than the ACE-FTS columns by an average of 14.4%. The ACE-FTS NO_2 partial columns are an average of 13.4% smaller than the total columns from the ground-based instruments, as expected. The ACE-MAESTRO NO_2 partial columns are larger than the total columns of the ground-based instruments by an average of 2.5% and are larger than the partial columns of the ACE-FTS by an average of 15.5%.

1 Introduction

The first three Canadian Arctic ACE (Atmospheric Chemistry Experiment) validation campaigns (the "Eureka campaigns") were held during polar sunrise at the Polar Environmental Atmospheric Research Laboratory (PEARL), 15 km from Eureka, Nunavut (80° N, 86° W) from 2004 to 2006. In 2004 and 2005, the lab was known as AStrO – the Arctic Stratospheric Ozone Observatory. All campaigns have involved a suite of six to seven ground-based

Correspondence to: A. Fraser
(amery@atmosp.physics.utoronto.ca)

Published by Copernicus Publications on behalf of the European Geosciences Union.

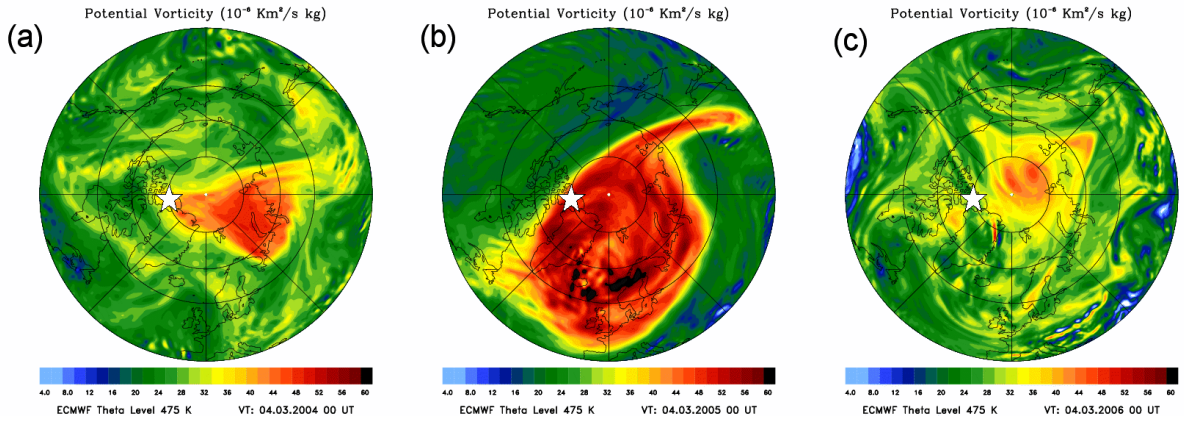

Fig. 1. ECMWF potential vorticity at 475 K potential temperature (about 19 km in the lower stratosphere) on 4 March **(a)** 2004, **(b)** 2005, and **(c)** 2006. The location of PEARL is indicated by the white star.

instruments, including three to four zenith-viewing UV-visible spectrometers. In 2004, these UV-visible instruments were: the University of Toronto Ground-Based Spectrometer (UT-GBS), the ground-based copy of the ACE-MAESTRO (ACE-Measurements of Aerosol Extinction in the Stratosphere and Troposphere Retrieved by Occultation) instrument onboard the ACE satellite, and the SunPhotoSpectrometer (SPS). In 2005 a Système d'Analyse par Observations Zénithales (SAOZ) instrument was added to the instrument suite. Detailed comparisons of the differential slant column densities (DSCDs) and vertical column densities (VCDs) of ozone and NO_2 measured by these four instruments have been performed and are discussed herein. These ground-based measurements are compared to partial columns measured by the ACE-FTS (ACE-Fourier Transform Spectrometer) and ACE-MAESTRO instruments onboard the ACE satellite. The behaviour of the ozone and NO_2 columns with respect to the location of the polar vortex is also discussed.

The zenith-sky DSCDs and VCDs are compared following the protocols established by the UV-visible Working Group of the Network for the Detection of Atmospheric Composition Change (NDACC) (Kurylo and Zander, 2000). In order to maintain the uniformity of measurements made throughout the NDACC, intercomparison campaigns between UV-visible instruments are periodically held. Three such campaigns have been held to date: in 1992 at Lauder, New Zealand (Hofmann et al., 1995), in 1996 at the Observatoire de Haute Provence, France (Roscoe et al., 1999), and in 2003 at the Andøya Rocket Range in Andenes, Norway (Vandaele et al., 2005). Roscoe et al. (1999) and Vandaele et al. (2005) present two methods of statistically comparing data from two zenith-viewing instruments, which have been adopted by the UV-visible Working Group for the validation of new instruments (Johnston et al., 1999). Although the Canadian Arctic ACE validation campaigns were not NDACC intercomparison campaigns, they did meet the requirements of an instrument intercomparison: the measurement site was reasonably free from tropospheric pollution, measurements were made for at least ten days, measurements were taken over the course of the entire day, and the measurements were coincident in time.

2 Description of the campaigns

The 2004 Canadian Arctic ACE Validation Campaign took place from 19 February to 15 April. Three UV-visible instruments (UT-GBS, MAESTRO, and SPS) were operated during the intensive phase, 19 February to 8 March. Only the UT-GBS remained for the extended phase of the campaign. Figure 1a shows the ECMWF (European Centre for Medium-Range Weather Forecasts) potential vorticity (PV) map at a potential temperature of 475 K ($\backsim$19 km) for 4 March. This level is in the lower stratosphere, where the peak in ozone mixing ratio is located. 2003/2004 was an unusual winter in the Arctic stratosphere, with a sudden stratospheric warming occuring in December 2003. The vortex began to recover in February, and reformed with a strong vortex in the middle and upper stratosphere. The vortex in the lower stratosphere did not recover substantially, as seen in Fig. 1a. The stratosphere did not undergo a final warming until late April (Manney et al., 2005, 2007a). Eureka was inside the vortex at those altitudes where it had reformed. The vertical columns from the intensive phase of this campaign have been previously discussed by Kerzenmacher et al. (2005).

The 2005 campaign ran from 18 February to 31 March. Four UV-visible instruments (UT-GBS, SAOZ, MAESTRO, and SPS) were operated during the intensive phase, with measurements beginning on 18 February and continuing to 8 March. During the extended phase, from 9 March to 31 March, only SAOZ and the UT-GBS remained in Eureka. The 2005 Arctic winter was notable for having the coldest

stratospheric temperatures on record. A major final warming of the stratosphere occurred on 10 March (Manney et al., 2007a). Figure 1b shows the ECMWF PV map at 475 K for 4 March. Eureka was on the edge of the polar vortex until early March, when the vortex began to move away and break apart.

The 2006 campaign took place from 17 February to 31 March. The same four UV-visible instruments as in 2005 were operated during both the intensive and extended phases of the campaign. 2006 was a warm winter in the polar stratosphere, with a sudden stratospheric warming occurring in January. As in 2004, the vortex began to reform in February, with a strong vortex (though not as strong as 2004) in the middle and upper stratosphere, and no substantial vortex in the lower stratosphere, as seen in Fig. 1c. The final warming of the stratosphere occurred in April (Manney et al., 2007a). As in 2004, Eureka was inside the vortex at altitudes where it had reformed.

A more complete view of the synoptic context of the three campaigns can be found in Manney et al. (2007a).

3 Instruments

The UT-GBS was assembled in 1998 and has since participated in seven polar sunrise campaigns at AStrO/PEARL (1999–2001, 2003–2007) (Bassford et al., 2005; Farahani, 2006; Farahani et al., 2008[1]). It consists of a triple-grating spectrometer with a thermo-electrically cooled, back-illuminated, 2048×512 pixel CCD (charged-coupled device) array detector. In 2004, an older CCD was used, which was 2000×800 pixels. Sunlight from the zenith-sky is gathered by a fused silica lens with a two-degree field-of-view, and focused on a liquid light guide, which minimises the effects of polarisation. Spectra are recorded continuously throughout the day, with varying exposure times to maximise the signal on the detector. Spectra were recorded between 345 and 560 nm, with a resolution of approximately 0.7 nm in the NO_2 region (400–450 nm) and 1.1 nm in the ozone region (450–550 nm). In 2004, an error in the data acquisition software caused a low signal-to-noise ratio, however, good data were still obtained. This error was corrected before the 2005 campaign. Also in 2004, data is missing between 15–23 and 25–29 of March due to a broken shutter in the spectrometer. The instrument is installed in a viewing hatch inside PEARL, under UV-transmitting plexiglas.

The SAOZ instrument was constructed in the late 1980s, and is now deployed in a global network for measurements of stratospheric concentrations of trace gases important to ozone loss (Pommereau and Goutail, 1988). SAOZ spectra were recorded between 270 and 620 nm, with a resolution of 1.0 nm. The detector is an uncooled 1024-pixel linear diode array. SAOZ records zenith-sky spectra with a ten-degree field-of-view. Spectra are recorded every fifteen minutes throughout the day, and continuously during twilight, defined as when the solar zenith angle (SZA) is between 80° and 95°. SAOZ is installed in a viewing hatch under a UV-transmitting plexiglas window. A SAOZ instrument has taken part in all three NDACC intercomparison campaigns.

MAESTRO is the ground-based clone of the grating spectrometer on board ACE (McElroy et al., 2007). MAESTRO is a double spectrometer, with two independent input optics, gratings, and detectors. The UV spectrometer has a spectral range from 260 to 560 nm and a resolution of 1.0 nm. The visible spectrometer has a spectral range from 525 to 1010 nm and a resolution of 2.0 nm. Both detectors are uncooled 1024-pixel linear diode arrays. The field-of-view is 0.1° by 6.5°. Only data from the UV spectrometer are used in this work.

SPS is the heritage instrument for MAESTRO. It is a photodiode array grating spectrometer that has been flown aboard the NASA ER-2 aircraft as the Composition and Photodissociative Flux Measurement (CPFM) experiment (McElroy, 1995). Zenith-sky spectra are recorded between 375 and 775 nm, with a resolution of 1.5 nm in both the ozone and NO_2 regions. The detector is an uncooled 1024-pixel linear photodiode array. Sunlight is collected by an achromatic lens, providing a 0.1° by 10° field-of-view. Although both MAESTRO and SPS are operated in direct Sun mode as well as zenith-sky mode, only the zenith-sky measurements will be discussed here. MAESTRO and SPS are mounted on a solar tracker on the roof of PEARL, which tracks the Sun in azimuth during zenith-sky viewing and in elevation and azimuth during direct Sun viewing. The instruments are outside, and are operated at near ambient temperature (generally between −30°C and −40°C).

The ACE satellite, also known as SCISAT-1, is a solar occultation satellite launched by the Canadian Space Agency in August 2003 (Bernath et al., 2005). The goal of the ACE mission is to improve the understanding of the chemical and dynamical processes that control the concentrations of ozone in the middle atmosphere. Two instruments make up the payload: the ACE-FTS and ACE-MAESTRO. ACE-FTS is an infrared Fourier transform spectrometer, with high resolution (0.02 cm^{-1}), operating from 750–4400 cm^{-1} (Bernath et al., 2005). The version 2.2 data set including updates for ozone, HDO, and N_2O_5 is used here (Boone et al., 2005). ACE-MAESTRO is a UV-visible-near-IR double spectrometer, with a resolution of 1.5–2.5 nm, and a wavelength range of 270–1040 nm. Version 1.2 is used here (McElroy et al., 2007). Only overpasses within 500 km of Eureka are considered; the distance is determined using the location of the occultation at the 30 km tangent point. Typical horizontal path lengths of the occultations are on the order of 500 km. Figure 2 shows the location of the satellite overpasses used

[1]Farahani, E., Strong, K., Mittermeier, R. L., and Fast, H.: Ground-based UV-visible spectroscopy of O_3, NO_2, and OClO at Eureka: Part I – Evaluation of the analysis method and comparison with infrared measurements, Atmos. Chem. Phys. Discuss., in preparation, 2008.

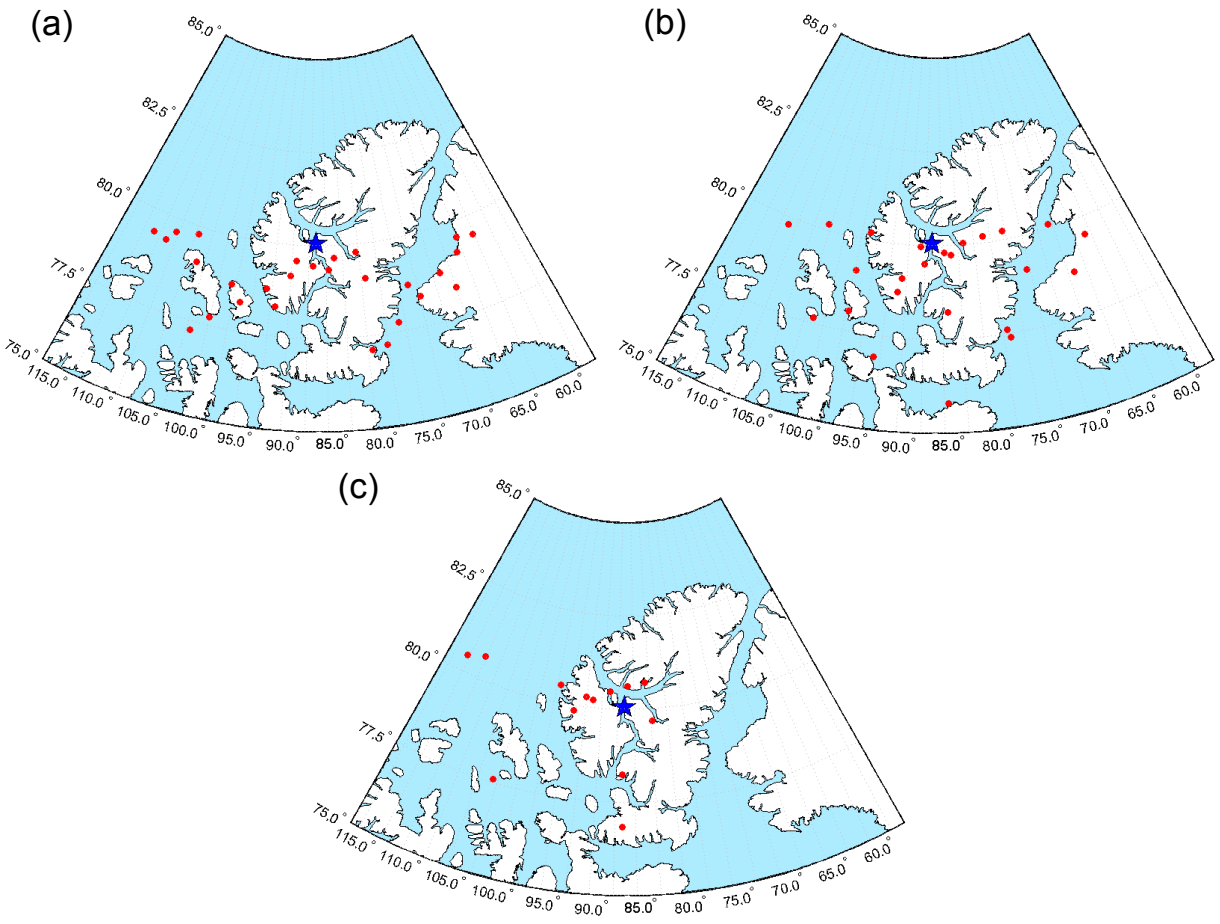

Fig. 2. Location of ACE tangent points at 30 km altitude within 500 km of PEARL in February and March **(a)** 2004, **(b)** 2005, and **(c)** 2006. All longitudes are North and all latitudes are West. The blue star indicates the location of PEARL.

in the comparisons. All of the overpasses are sunset occultations.

Ozonesondes are launched weekly at the Eureka weather station (Tarasick et al., 2005). During the intensive phase of all three campaigns, ozonesondes were launched daily. Generally the ozonesondes are launched at 23:15 UTC (18:15 LT), however, on occasion, the launch time was altered to match a satellite overpass.

4 Data analysis and comparison method

4.1 Differential optical absorption spectroscopy

In this work, the DOAS technique (Differential Optical Absorption Spectroscopy) (e.g., Solomon et al., 1987; Platt, 1994) is used for the analysis of spectra from all four instruments with absorption cross-sections of ozone (Burrows et al., 1999), NO_2 (Vandaele et al., 1998), H_2O (converted from the line parameters given in Rothman et al., 2003), O_4 (Greenblatt et al., 1990), and the Ring pseudo-absorber (Chance and Spurr, 1997) fitted using a Marquardt-Levenberg non-linear least-squares technique. DSCDs of ozone are retrieved between 450 and 550 nm, and NO_2 DSCDs are retrieved between 400 and 450 nm.

The program WinDOAS, developed by IASB-BIRA (Belgian Institute for Space Aeronomy, Fayt and Van Roozendael, 2001), has been used to analyse data from all four instruments. In this way, differences in the DSCDs should be a result of the spectra themselves and not an artefact of different analysis procedures. Table 1 gives the details of the WinDOAS settings used for the four instruments. These settings were chosen to optimise the fits from the instruments. For MAESTRO and SPS it was necessary to perform a separate calibration for the ozone and NO_2 regions. For SAOZ and UT-GBS one calibration was sufficient. The Gaussian slit function is fit in each of the calibration subwindows and is used to smooth the high-resolution cross-sections to the resolution of the instrument. The wavelength calibration is performed on both the reference and twilight spectra.

Table 1. Details of the WinDOAS retrievals for the four UV-visible instruments. The same settings are used for each year of analysis. The same polynomial degree is used in the calibration for both the wavelength shift and slit function parameters, and is given in the column CPD (calibration polynomial degree). The continuous function is the degree of the polynomial fit to the optical depth in the DOAS analysis.

Instrument	Species	Slit Function	CPD	Calibration Window Limit (nm)	Number of Subwindows	Continuous Functions	Offset
UT-GBS	Ozone	Gaussian	3	400–550	5	0,1,2,3	none
UT-GBS	NO_2	Gaussian	3	400–550	5	0,1,2,3	none
SAOZ	Ozone	Gaussian	3	400–550	4	0,1,2,5	linear
SAOZ	NO_2	Gaussian	3	400–550	4	0,1,2,5	none
MAESTRO	Ozone	Gaussian	3	400–550	5	0,1,2,3	none
MAESTRO	NO_2	Gaussian	2	400–450	3	0,1,2,3,4,5	none
SPS	Ozone	Gaussian	3	400–550	4	0,1,2,3,4,5	linear
SPS	NO_2	Gaussian	2	400–450	3	0,1,2,3,4,5	linear

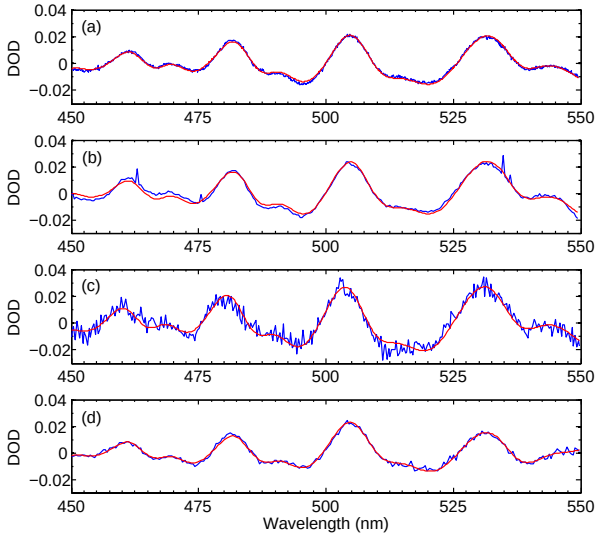

Fig. 3. Typical differential optical depth (DOD) ozone fits for **(a)** UT-GBS, **(b)** SAOZ, **(c)** MAESTRO, and **(d)** SPS. All fits are for the afternoon of 4 March 2005 at a SZA of approximately 90°. In all plots, the blue line is the data, while the red line is the fit to the data.

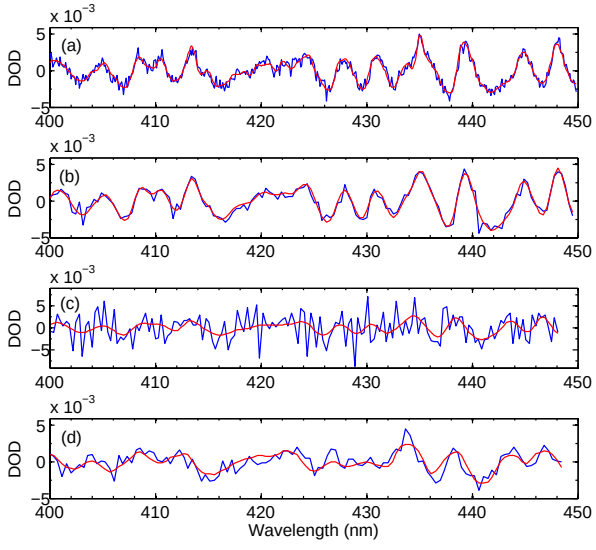

Fig. 4. As Fig. 3, but for NO_2. Note the different scale for MAESTRO.

The degree of the polynomial fit to the optical depth in the DOAS analysis is given by the continuous function. To correct for stray light in the instrument, an offset can be fitted.

Daily reference spectra were used, with SZAs varying from 90.8° for the earliest day of the campaign (20 February) to 70.3° for the last day of the campaign (14 April). If the reference spectra of two instruments differ by more than 0.5° that day was not included in the comparisons. This eliminated fewer than five comparisons from each campaign.

Figure 3 shows typical ozone spectral fits from the four instruments for 4 March 2005. Figure 4 shows typical NO_2 spectral fits for the same day. Fits from all years are comparable for all instruments. For both species, the MAESTRO spectral fits are noisier than those from the other instruments. This is because the other instruments average spectra before they are analysed. For the UT-GBS and SAOZ, the number of spectra that are averaged is variable (4–300 for the UT-GBS, 1–115 for SAOZ), and is limited by the maximum time taken to record the spectra, to avoid smearing over large SZAs. SPS averages two spectra before they are analysed. MAESTRO records individual spectra. In this work, MAESTRO DSCDs are averaged over 0.25° intervals. Individual integration times range between 13 ms and 30 s for the UT-GBS, between 0.5 s and 19 s for SAOZ, and between 50 ms and 10 s for MAESTRO and SPS. The NO_2 DOD fits for SPS and MAESTRO are poorer than the fits from the

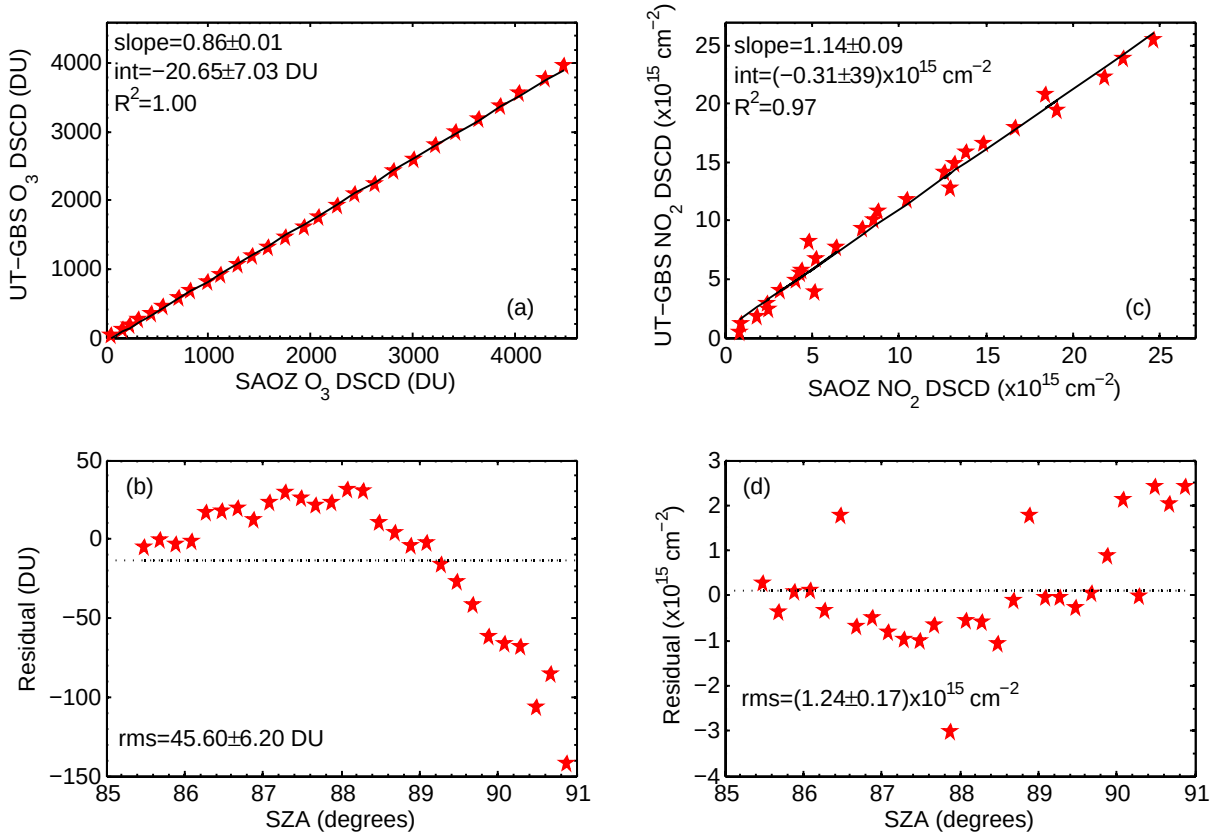

Fig. 5. **(a)** Type 1 regression analysis for ozone between the UT-GBS and SAOZ for 4 March 2005, **(b)** residuals of the fit in (a), **(c)** same as (a) but for NO_2, and **(d)** same as (b) but for NO_2. In (a) and (c) the solid lines are the results of the regression fit. In (b) and (d) the dashed lines are the average residuals of the regression fit.

UT-GBS and SAOZ. The Eureka campaigns take place just after polar sunrise, when the NO_2 column is very small. The NO_2 is near the limits of detection of SPS and MAESTRO.

4.2 Derivation of vertical column densities

The primary quantity derived from the zenith-sky measurements is the DSCD as a function of solar zenith angle. In order to convert the measurements of DSCD into VCD, the use of an air mass factor is required. In this work, daily air mass factors (AMFs) are calculated using a radiative transfer model initialized with temperature, pressure, and ozone profiles taken from the ozonesondes flown on that day and NO_2 profiles taken from a chemical box model at 75° N in February or March (McLinden et al., 2002). If no ozonesonde is available, the nearest sonde to that day is taken. NO_2 is allowed to vary along the path of light, using the diurnal variation from the chemical box model. DSCDs are related to the VCD and the AMF by Eq. (1):

$$\mathrm{DSCD(SZA)=VCD(SZA)\times AMF(SZA)-RCD.} \quad (1)$$

RCD is the reference column density, and is the amount of absorber in the reference spectrum used in the DOAS analysis.

Two methods are used to convert ozone DSCDs to VCDs. In the first method, or Langley plot method, a Langley plot of DSCD between 86° and 91° versus AMF is made. From Eq. (1), the VCD can be found by finding the slope of the Langley plot. The Langley plot will only be a straight line if the AMFs are correct, if the ozone is constant through the twilight period, and if the ozone field is homogenous. In the second method, or averaging method, a Langley plot of DSCD between 86° and 91° versus AMF is made. From Eq. (1), the RCD can be found by taking the ordinate of the Langley plot. The RCDs from the morning and afternoon are averaged to give one RCD for each day. Each individual DSCD is then converted to a VCD using Eq. (1). The average VCD for one twilight period is found by averaging the VCDs between 86° and 91°. The two methods should yield the same results, provided the Langley plot is a straight line (Sarkissian et al., 1997).

There are also two methods to convert NO_2 DSCDs to VCDs. The averaging method can be used, or the VCD at

Table 2. Sources of measurement errors. Values in brackets in the UT-GBS column refer to the UT-GBS in 2004, which had a different detector than in 2005–2006, as well as an error in the data acquisition code.

	UT-GBS		SAOZ		MAESTRO		SPS	
Source of error	O_3	NO_2	O_3	NO_2	O_3	NO_2	O_3	NO_2
Random noise	1(2.5)%	2(3)%	1%	2%	2.5%	3%	1%	3%
Instrument error (dark current, bias, slit function)	1(2)%	1(2)%	1%	1%	1%	1%	1%	1%
Pseudo-random errors	1–2%	4–6%	1–2%	4–6%	1–2%	4–6%	1–2%	4–6%
Absolute cross-sections	2.6%	5%	2.6%	5%	2.6%	5%	2.6%	5%
Temperature dependence of NO_2 cross-section	–	<8%	–	<8%	–	<8%	–	<8%
Filling in of absorption by Raman scattering	1%	5%	1%	5%	1%	5%	1%	5%
Total rms DSCD error	3.5(4.6)%	12.0(12.6)%	3.5%	12.0%	4.2%	12.2%	3.5%	12.2%
AMF error	2%	5%	2%	5%	2%	5%	2%	5%
Uncertainty in RCD	1%	10%	1%	10%	1%	15%	3%	15%
Total rms VCD error	4.1(5.0)%	16.4(16.8)%	4.1%	16.4%	4.8%	20.0%	5.0%	20.0%

90° can be found using the DSCD at 90° and Eq. (1). The RCD is found by making a Langley Plot of DSCDs between 86° and 91°. Ideally, SZAs from 80° to 85° would be used, but these are not available for many days during the campaigns. The RCDs from both twilight periods are averaged to give a daily RCD. For NO_2, the results from each method are slightly different, due to the diurnal variation of NO_2, with the averaging method yielding an average VCD between 86° and 91°, and the 90° method yielding a VCD at 90°.

Measurement errors are calculated from the root-sum-square (rms) of individual sources of error, after Bassford et al. (2005) and references therein. For DSCDs, they include random noise on the spectra, instrument error arising from uncertainties in the dark current, bias, and slit function, pseudo-random errors resulting from unaccounted-for structure in the spectra, errors in the absorption cross-sections, the temperature dependence of the NO_2 cross section, and the effects of Raman scattering, which fills in the absorption lines. For VCDs, they also include error in the air mass factors and uncertainty in the reference column density. The individual and total errors are shown in Table 2.

4.3 Comparison methods

The ground-based instruments are all zenith-viewing, and therefore share the same viewing geometry, although not the same field-of-view. The DSCDs can be compared as described in Johnston et al. (1999). Two types of certification are defined by NDACC. Type 1 standards apply to instruments that are certified for global studies and trend measurements. The DSCDs from two instruments are transformed onto a common SZA grid ranging from 75° to 91°, and then a linear regression analysis is performed. In this work, on days when the Sun did not reach 75°, the minimum SZA was used. The slope of the regression fit represents how well the two data sets agree: a non-unity slope indicates that the DSCDs diverge. A non-zero ordinate represents a systematic offset between the two data sets. Residuals are also calculated. Large residuals are a sign of scatter in at least one of the data sets. The linear regressions are performed following the method of York et al. (2003), which is a least-squares estimation method. The following targets have been set for the campaign mean of these parameters: slope=(0.97–1.03), intercept=±55.8 DU (Dobson Units), and root-mean-square of the residuals <37.2 DU for ozone and slope=(0.95–1.05), intercept=$\pm 1.5\times10^{15}$ molec/cm^2, and residuals $<1.0\times10^{15}$ molec/cm^2 for NO_2. An example of the Type 1 regression analysis is shown in Fig. 5 for 4 March 2005 between the UT-GBS and SAOZ. The increasing residuals seen in Fig. 5b are typical of DSCDs that were analysed in different wavelength regions. This is not the case for this comparison, and this feature is common to all UT-GBS vs. SAOZ comparisons performed for Eureka. This is possibly due to the differing fields-of-view of the instruments, the effect of which is further discussed in Sect. 5.1.

Instruments that meet Type 2 standards are certified for process studies and satellite validation. In this comparison, the VCDs over the course of a twilight are transformed onto a common SZA grid ranging from 85° to 91° and the mean of the ratio of the data from the two instruments is taken. For ozone, the campaign mean of the ratio should be between 0.95 and 1.05, with a standard deviation (one sigma) less than 0.03. For NO_2, the mean of the ratio should be between 0.90 and 1.10, with a standard deviation (one sigma) less than 0.05. Figure 6 shows an example of this comparison for 4 March 2005 between the UT-GBS and SAOZ. Since NO_2 has a diurnal variation, the offset between the morning and afternoon VCDs can be calculated by finding the y-intercept of a plot of the afternoon VCDs against the morning VCDs. If the diurnal variation of the species is roughly constant over the campaign, the standard deviation in this offset over the duration of the campaign should be

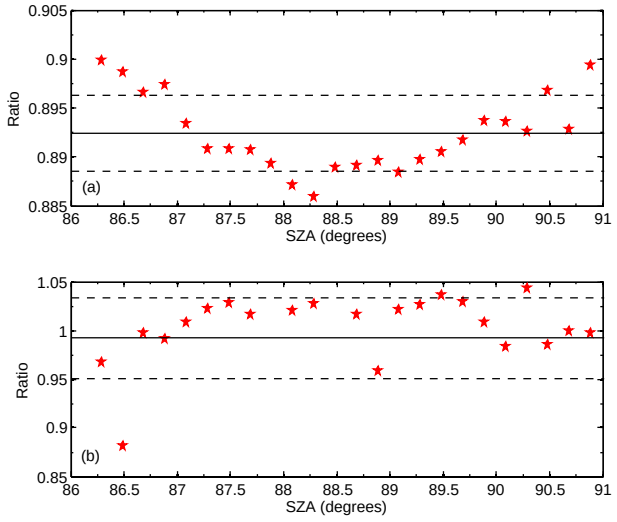

Fig. 6. **(a)** Type 2 comparisons for ozone between UT-GBS and SAOZ for 4 March 2005. The solid line indicates the mean of the ratio between the two instruments, while the dashed lines show the extent of the standard deviation. **(b)** same as (a) but for NO_2.

less than 2.5×10^{15} molec/cm^2. However, for polar measurements, the amount of sunlight varies significantly from day to day, meaning the diurnal variation is not constant, and so the offset is not expected to be constant. Because of this, the offset is not discussed herein.

5 Differential slant column density comparisons

5.1 Ozone

Figure 7 shows the DSCDs for the four ground-based instruments on 4 March 2004–2006. The general agreement between all the instruments is good up to 92°. At this point the MAESTRO and SAOZ DSCDs begin to diverge from the other instruments. In the case of SAOZ, the divergence is always to lower DSCDs. This divergence is due to the consistently warm temperatures (25–30°C) inside the viewing hatch of the instrument. The data beyond 92° is unreliable due to the dark signal (which includes the thermal noise) making up a larger percentage of the total signal. The MAESTRO DSCDs diverge to both higher and lower DSCDs, depending on the twilight period. There seems to be no relation between which way the DSCDs diverge and the outside temperature or cloudiness of the day. As only SZAs up to 91° are used in the DSCD comparisons and in the calculation of VCDs, these divergences will not affect the comparisons to be discussed.

Figure 8 shows the results of the Type 1 ozone DSCD comparisons. In all figures, the campaign-averaged parameter is given, with the standard error ($\sigma/\sqrt{N}$, σ is the standard deviation, N is the number of comparisons) represented as the error bars. Table 3 gives the number of twilight periods averaged in each of the comparisons. No MAESTRO vs. SPS comparison is given for the 2004 campaign due to the small number of twilight periods available for comparison (less than three).

Table 3. Number of twilight periods used in the campaign averages for ozone and NO_2 for both Type 1 and 2 comparisons.

		O_3		NO_2	
Comparison	Year	AM	PM	AM	PM
UT-GBS vs. SAOZ	2005	29	30	29	30
	2006	30	34	29	29
UT-GBS vs. SPS	2004	5	3		
	2005	9	9	8	8
	2006	17	23	10	18
UT-GBS vs. MAESTRO	2004	3	3		
	2005	6	7		
	2006	17	14	10	10
SPS vs. SAOZ	2005	8	10	6	7
	2006	16	23	13	22
MAESTRO vs. SAOZ	2005	7	9		
	2006	15	17	10	9
MAESTRO vs. SPS	2005	6	8		
	2006	11	10	8	10

Examining the slopes first, 16 of the 28 values (seen in Fig. 8a, d, and g) meet the NDACC standards, and a further three meet the standards within the error bars. The comparisons in 2004 and 2006 are similar, with the exception of the UT-GBS vs. SPS afternoon comparisons. It should be noted that the 2004 comparison has only three data points. The NDACC requires at least ten days of comparisons to ensure proper statistics. The comparisons tend to be worse in 2005, especially the UT-GBS vs. SAOZ comparison. As discussed in Sect. 2, Eureka was located on the edge of the polar vortex throughout most of the campaign. SAOZ has a significantly larger field-of-view than the UT-GBS (10° vs. 2°). Because of this, SAOZ will view more of the atmosphere than the UT-GBS. With the heterogenous ozone field expected due to Eureka's position on the edge of the vortex, the discrepancy in DSCDs is likely a result of the instruments sampling different portions of the atmosphere. The sizes of the fields-of-view of MAESTRO and SPS are between those of the UT-GBS and SAOZ, so the effect is not expected to be as large. No pairs of instruments meet the NDACC standards for both twilight periods in all years of comparison, however the UT-GBS vs. SAOZ comparisons consistently do not meet

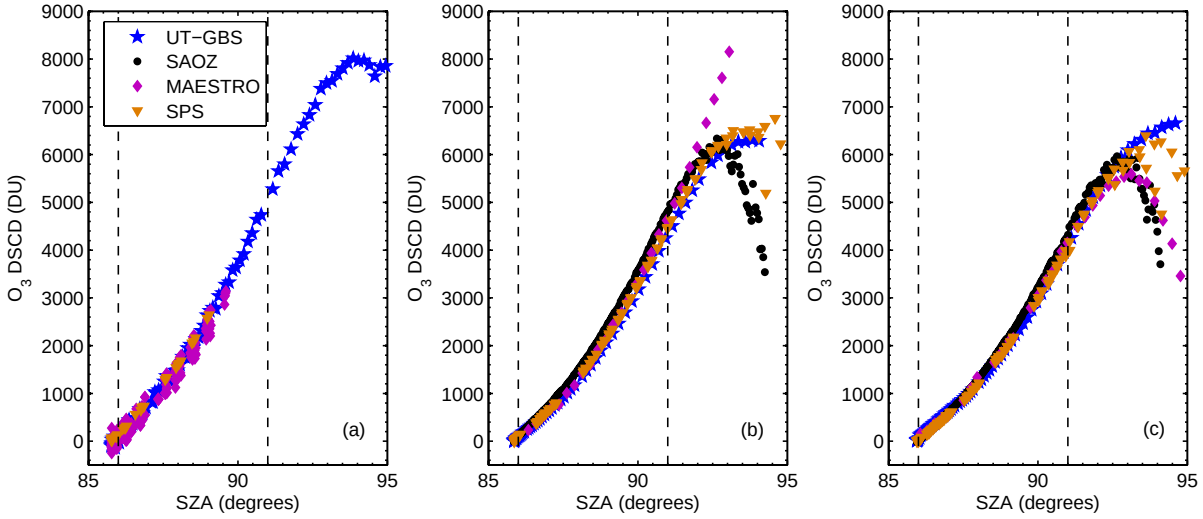

Fig. 7. Ozone differential slant column densities for the UV-visible instruments for the afternoon of 4 March of **(a)** 2004, **(b)** 2005, and **(c)** 2006. The dashed lines at 86° and 91° indicate the range of DSCDs used in the calculation of VCDs. For the Type 2 comparisons, DSCDs between 85° and 91° are used. For the Type 1 comparisons, all DSCDs up to 91° are used.

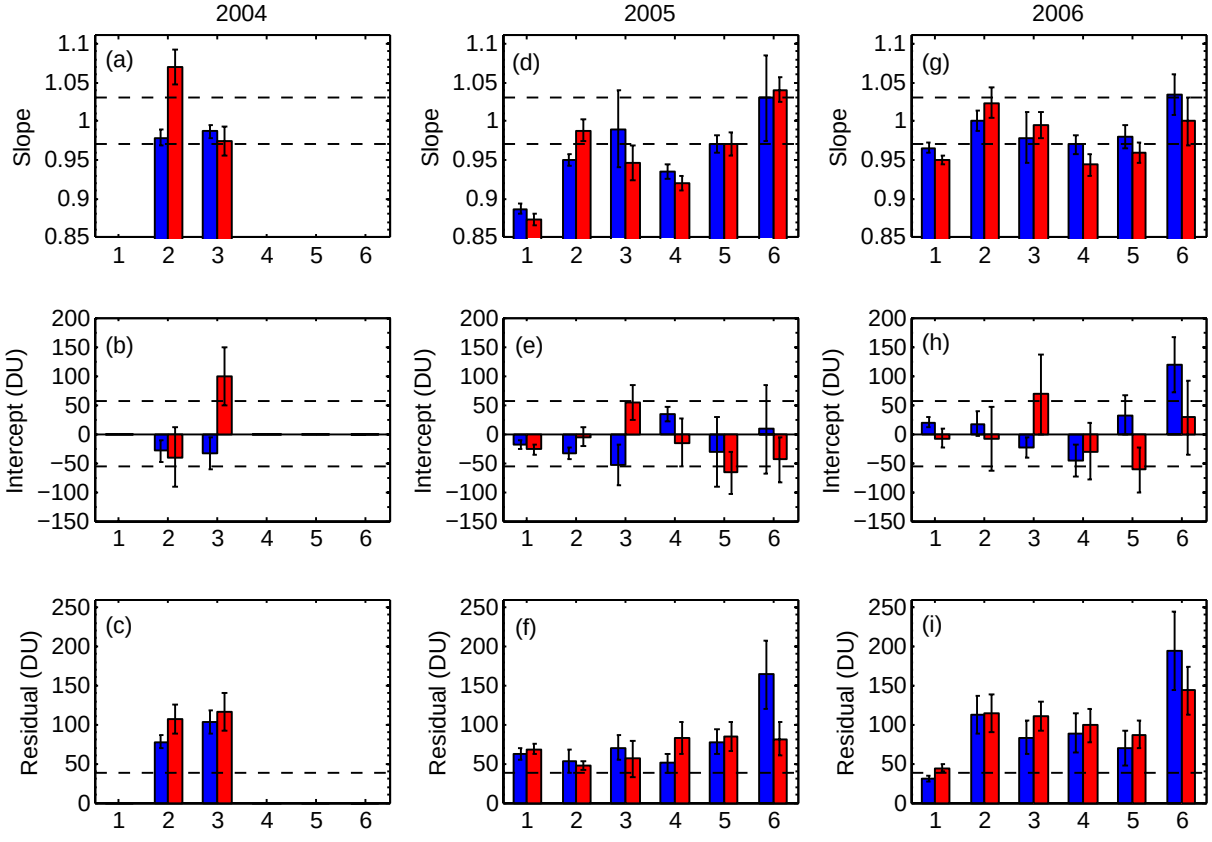

Fig. 8. Ozone DSCD Type 1 results for **(a–c)** 2004, **(d–f)** 2005, and **(g–i)** 2006. In all figures, blue represents the morning comparisons, while red represents the afternoon. Error bars indicate the standard error. Dashed lines indicate the NDACC standards. The numbers represent the comparisons between the different instruments: 1 – UT-GBS vs. SAOZ, 2 – UT-GBS vs. SPS, 3 – UT-GBS vs. MAESTRO, 4 – SPS vs. SAOZ, 5 – MAESTRO vs. SAOZ, 6 – MAESTRO vs. SPS.

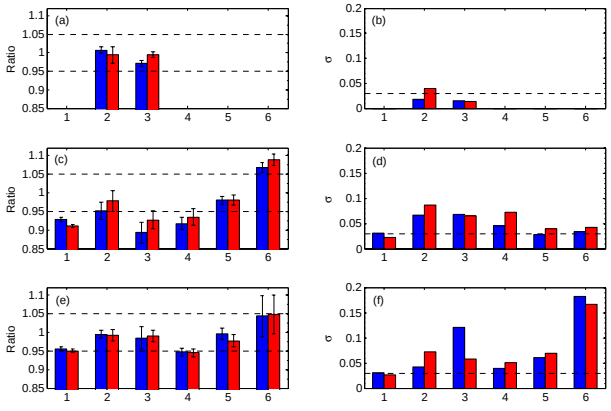

Fig. 9. Ozone Type 2 ratio results for **(a)** 2004, **(c)** 2005, and **(e)** 2006. The error bars represent the standard error. The standard deviation results for **(b)** 2004, **(d)** 2005, and **(f)** 2006. The dashed lines indicate the NDACC standards. Colours and numbers represent the same comparisons as Fig. 8.

the slope standards. The UT-GBS vs. MAESTRO comparisons meet the NDACC standards within the error bars each year; the only twilight period that does not meet the standards is the 2005 afternoon, where there are just seven days to compare. Generally, comparisons with SPS and MAESTRO improve in 2006 when these instruments participated in the extended phase of the campaign.

For the average intercepts, in Fig. 8b, e, and h, 23 of the 28 comparisons meet the NDACC standards, and a further four comparisons agree within the error bars. For comparisons involving SPS and MAESTRO, the standard errors are large compared to the average intercepts. The UT-GBS vs. SAOZ, UT-GBS vs. SPS, and SPS vs. SAOZ comparisons consistently meet the NDACC standard for both twilight periods for all years of comparison. The average residuals (Fig. 8c, f, and i) are all much larger than the NDACC standard, with large standard error, with the exception of the UT-GBS vs. SAOZ 2006 comparison. As discussed in Sect. 4.3, large residuals are an indication of scatter in at least one of the data sets.

The campaign-averaged results of the Type 2 ozone comparisons are shown in Fig. 9. In 2004 and 2006, most of the ratios agree with the NDACC standards, or are slightly outside the range (e.g. the SPS vs. SAOZ 2006 comparisons). In 2005, the UT-GBS vs. SAOZ, UT-GBS vs. MAESTRO, SPS vs. SAOZ, and MAESTRO vs. SPS comparisons are all outside the range, although some of these comparisons agree within the error bars. In Fig. 8, the corresponding comparisons generally have slopes that do not meet the NDACC standards, and intercepts that do. As discussed above, this discrepancy may be due to Eureka's position on the edge of the polar vortex during much of the campaign, and the difference in fields-of-view of the instruments.

The standard deviations of the ratios for the campaign are also shown in Fig. 9. Most of the standard deviations are larger than the requirement, the exceptions being the UT-GBS vs. SAOZ comparisons for all years, the UT-GBS vs. MAESTRO 2004 comparison, the morning of the UT-GBS vs. SPS 2004 comparison, and the morning of the SPS vs. SAOZ 2005 comparison. This is an indication of the consistency of the ratio comparisons – small standard deviations mean that the ratio has a smaller spread of values. The standard deviations for comparisons involving SPS and MAESTRO are, in general, larger in 2006 than in 2005. This is likely a result of these instruments participating in the extended campaign. As the light levels increased towards the end of March, both instruments recorded many more saturated spectra than during the intensive phase. As a result there are fewer DSCDs for these instruments. The regression parameters for comparisons involving MAESTRO and SPS during the extended phase are more scattered than during the intensive phase. If only the intensive phase is considered, the standard deviations are smaller.

5.2 NO_2

Figure 10 shows the NO_2 DSCDs from the four ground-based instruments for 4 March 2004–2006 (the same day as in Fig. 7). The UT-GBS DSCDs from 2004 are much more scattered than those in the other years, as a result of the low signal-to-noise ratio discussed in Sect. 3. In all years, there is more scatter in the data, and a greater discrepancy is seen between the instruments than for the ozone DSCDs. In 2004, the SPS and MAESTRO DSCDs are roughly the same at noon, and are within the large scattered range of the UT-GBS. At high SZAs, the DSCDs from the three instruments diverge. In 2005–2006, the agreement between all instruments is good at lower SZAs, and the DSCDs begin to diverge at higher SZAs. The MAESTRO and SPS DSCDs are more scattered than those of the other instruments for all SZAs. In 2005, the UT-GBS and SAOZ DSCDs agree, while the SPS and MAESTRO DSCDs are smaller. In 2006, the DSCDs from SPS and MAESTRO are scattered about the DSCDs from the UT-GBS and SAOZ. The SAOZ DSCDs become scattered above 92°, a result of the higher thermal noise contribution discussed in Sect. 5.1. Only SZAs up to 91° are used in the comparisons.

Figure 11 shows the results of the Type 1 comparisons for NO_2 for the 2005–2006 campaigns. The error bars represent the standard errors. No comparisons are shown in 2004 due to the small number of comparisons for this year (less than three), as well as the large amount of scatter on the DSCDs from the UT-GBS. No NO_2 comparisons from MAESTRO are shown in 2005 due to the small number of twilight periods available for comparison. The number of twilight periods used in the averages is given in Table 3.

Eleven of the 16 campaign-averaged slopes agree with the NDACC standards, and an additional one agrees within error

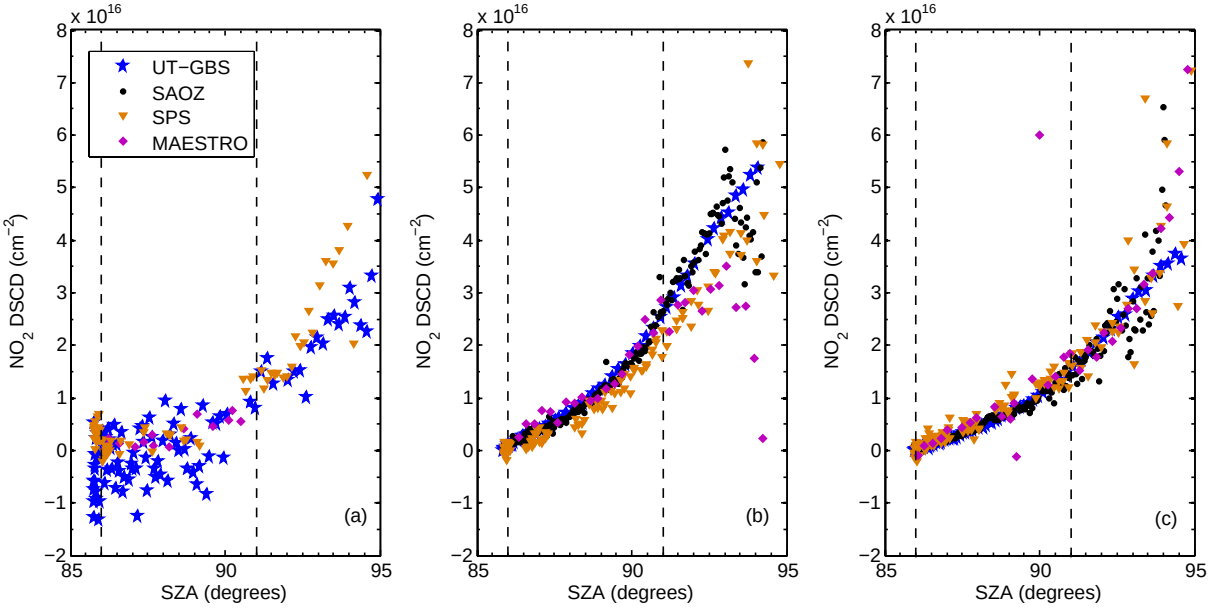

Fig. 10. NO_2 differential slant column densities for the UV-visible instruments for the afternoon of 4 March of **(a)** 2004, **(b)** 2005, and **(c)** 2006. The dashed lines at 86° and 91° indicate the range of DSCDs used in the calculation of VCDs. For the Type 2 comparisons, DSCDs between 85° and 91° are used. For the Type 1 comparisons, all DSCDs up to 91° are used.

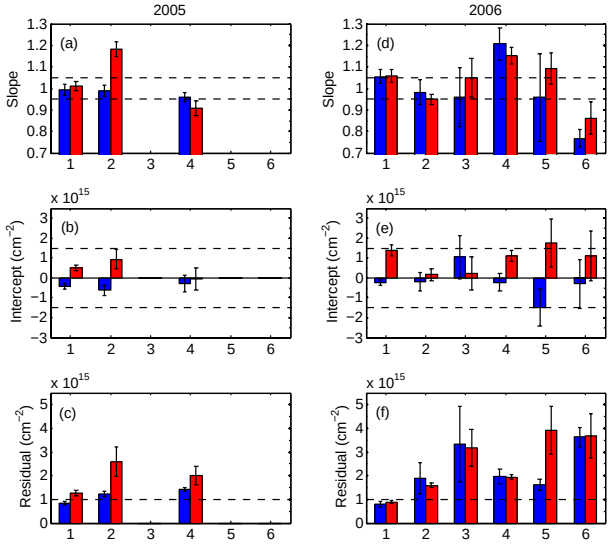

Fig. 11. NO_2 DSCD Type 1 results for **(a–c)** 2005, and **(d–f)** 2006. Dashed lines indicate the NDACC standards. In all figures, blue represents the morning comparisons, while red represents the afternoon. Error bars indicate the standard error. The numbers represent the comparisons between the different instruments: 1 – UT-GBS vs. SAOZ, 2 – UT-GBS vs. SPS, 3 – UT-GBS vs. MAESTRO, 4 – SPS vs. SAOZ, 5 – MAESTRO vs. SAOZ, 6 – MAESTRO vs. SPS.

bars. The UT-GBS vs. SAOZ comparison meets the standard for both twilight periods for both years of comparison. No pair of instruments consistently fails to meet the NDACC standards. In general, the standard errors of the morning slopes are larger than those of the afternoon slopes, a result of the smaller amount of NO_2 in the morning versus the afternoon.

For the campaign-averaged intercepts, 17 of the 18 comparisons meet the NDACC standards, while the remaining comparison meets the standard within the error bars. As with the slope values, the standard errors are generally larger in the morning than in the afternoon. The campaign-averaged residuals for the UT-GBS vs. SAOZ comparison meet or are close to the NDACC standards in both years. The other residuals, however, are up to four times larger than the standard. This is a reflection of the scatter in the DSCDs discussed above.

The results of the Type 2 NO_2 comparisons are shown in Fig. 12. All but two of the ratio results meet the NDACC standard. One of these, the MAESTRO vs. SPS 2006 morning comparison, is very close with a large error bar. The other, the UT-GBS vs. SPS comparison, is large and does not agree within the error bars. The slope for this pair in the Type 1 comparisons shown in Fig. 11 is also large.

The standard deviations of the ratios for the campaign are also shown in Fig. 12. All of the standard deviations are up to nine times the NDACC standard. This is a reflection of the scatter in the DSCDs, and hence the VCDs. The NDACC standards were established after a summer-time mid-latitude

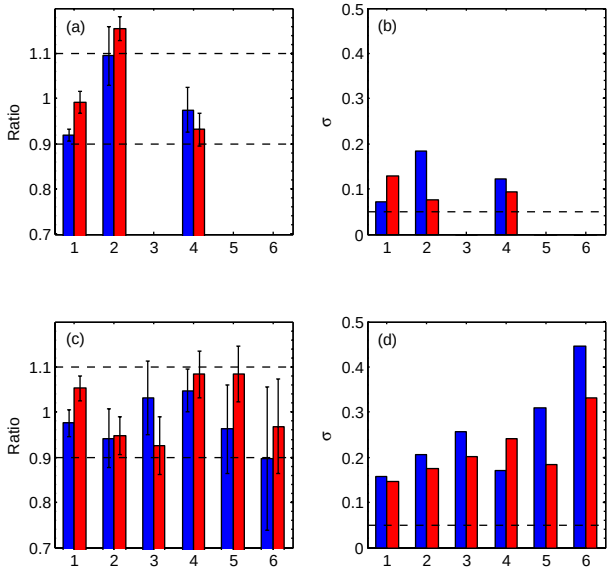

Fig. 12. NO_2 Type 2 ratio results for **(a)** 2005, and **(c)** 2006. The error bars are the standard deviations. The standard deviations are shown in **(b)** for 2005 and **(d)** for 2006. The dashed lines indicate the NDACC standards. Colours and numbers represent the same comparisons as Fig. 11.

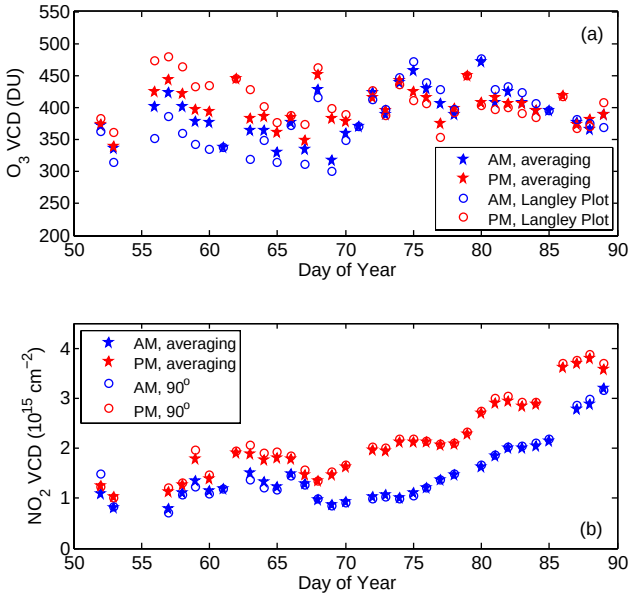

Fig. 13. **(a)** Comparison of the averaging and Langley plot methods for finding the ozone VCD for the UT-GBS in 2005. **(b)** Comparison of the averaging and 90° methods for NO_2.

intercomparison campaign, when NO_2 is at its annual peak. There is significantly less NO_2 in the polar springtime Arctic stratosphere, making it more difficult to detect, and therefore increasing the random noise (scatter) on the DSCDs.

5.3 Relation to the previous MANTRA 2004 comparison

The UT-GBS, SAOZ, MAESTRO, and SPS instruments all took part in the Middle Atmosphere Nitrogen TRend Assessment (MANTRA) campaign in Vanscoy, Saskatchewan (52° N, 107° W) in late summer 2004. The results from this comparison were discussed by Fraser et al. (2007). For the MANTRA Type 1 ozone comparison, the slopes were found to agree with the NDACC standards for the MAESTRO vs. SPS comparisons. The morning slopes for the UT-GBS vs. SPS and MAESTRO vs. SAOZ comparisons also met the NDACC standards. The UT-GBS vs. SPS afternoon and both UT-GBS vs. MAESTRO comparisons agreed with the standards within the standard error. The intercepts were universally large, two to four times the NDACC standards, with large standard error, and the residuals were large: up to three times the NDACC standard.

For the ozone Type 1 analysis for the Eureka campaigns, the slopes and residuals found here are consistent with the slopes and residuals found during the MANTRA campaign. The intercepts for the Eureka campaigns are much smaller than those found during MANTRA. A daily reference spectrum was used for the DOAS analysis in the Eureka campaigns, while a single reference spectrum was chosen for the MANTRA campaign. Daily reference spectra may cause more consistent intercepts since shifts in the wavelength calibration can occur over the course of a campaign for an instrument due to changes in the temperature. Since the diurnal changes in the wavelength calibration are in general smaller than the changes over a campaign, using a daily reference spectrum can result in better calibration for the DOAS analysis, and thus more accurate DSCDs at lower SZAs. The wavelength shifts determined by WinDOAS for the Eureka spectra are generally small, between 0 and 0.2 pixels through one twilight period, while the shifts determined by WinDOAS for the MANTRA spectra vary between 0 and 3 pixels, depending on the day. Over one twilight period during MANTRA, the variation can be as high as 0.8 pixels.

The MANTRA Type 2 ozone comparisons had the morning UT-GBS vs. SAOZ, UT-GBS vs. MAESTRO, and morning MAESTRO vs. SAOZ ratios all meeting the NDACC standards, while the other comparisons were close to the desired range. The SPS vs. SAOZ comparisons were significantly smaller than the standards. The standard deviations for all comparisons, with the exception of the UT-GBS vs. SAOZ morning, were within the standards. The ozone Type 2 ratios presented here are better than those found during the MANTRA campaign: the ratios mostly meet the NDACC standards. The standard deviations are larger than during MANTRA, most likely due to the larger spatial and diurnal variability in the spring polar ozone field versus the summer mid-latitude ozone field.

Only NO_2 data from the UT-GBS and SAOZ were presented in Fraser et al. (2007). For the Type 1 comparisons, the slopes met the NDACC standards. The morning intercept was 3.5 times larger than required, while the afternoon intercept was 1.25 times larger than the standard. The residuals were three to four times larger. In the comparisons for Eureka for the UT-GBS and SAOZ, all three parameters meet the NDACC standards in 2006. In 2005, only the afternoon residual does not meet the standard. The improved comparisons are a result of the improved signal-to-noise ratio of the UT-GBS after the MANTRA 2004 campaign, when the error in the data acquisition code was discovered and a new CCD was obtained.

For the Type 2 NO_2 comparisons, the NDACC standards were met in the MANTRA comparison, with the exception of the morning standard deviation. In the Eureka comparison, the ratios meet the NDACC standard, while the standard deviations do not. This is likely due to low NO_2 concentrations and atmospheric variability of the springtime polar atmosphere.

6 Vertical column density comparisons

6.1 Comparison of methods

As discussed in Sect. 4.2, there are two methods for calculating both the ozone and NO_2 vertical column densities. Figure 13 shows the results of both of these methods for both species in 2005 for the UT-GBS instrument only. Both methods have been used on the other four instruments as well, and the differences between the methods are similar. This year is shown because Eureka spent the beginning of the campaign on the edge of the polar vortex. After March 8 (day 67), the vortex moved away from Eureka and began to break up (Manney et al., 2007a).

The ozone results, shown in Fig. 13a, show poor agreement between the two methods to day 67, and good agreement between the VCDs after this day. The discrepancies between the methods can be as high as 50 DU (or ∽15% of the total column) during the first half of the campaign, while the differences are no greater than 20 DU (or ∽6% of the total column) during the second half. While Eureka was on the edge of the vortex, due to the viewing geometry of the instrument, the air masses sampled in the morning were towards the east into the vortex, while the air masses sampled in the afternoon were towards the west, out of the vortex (see Fig. 1). The SZA range used for both methods is 86° to 91°. Both methods of finding the ozone VCD assume that the VCD does not change over the twilight period. This assumption is not valid for the period that Eureka was on the edge of the vortex, because each DSCD is in fact sampled at a different physical location. The measurements closest to noon are south of Eureka, while those near a SZA of 90° are to the East or the West, either into the vortex in the morning or away from the vortex in the afternoon. Figure 14 shows the geometrical projection of the ozone maximum (taken to be 18 km) along the line of sight to the Sun for 4 March 2005. Because there are more measurements taken at solar noon, the averaging method weights the VCD towards these noontime measurements. For this period of the campaign, this results in larger VCDs in the morning and smaller VCDs in the afternoon. During the second part of the campaign, when the vortex had moved away from Eureka, the methods agree, as a result of the more homogenous ozone field.

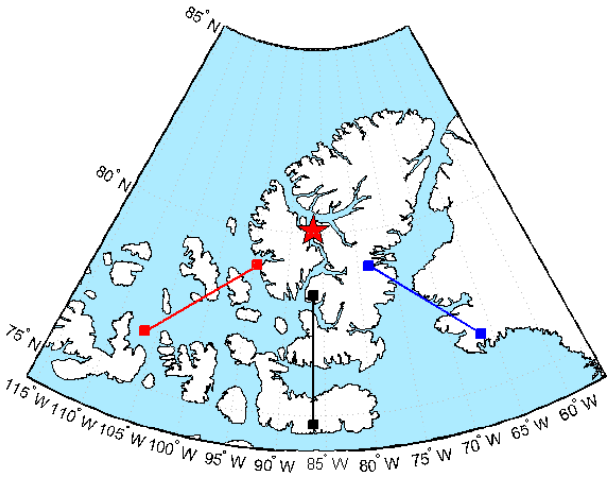

Fig. 14. Spatial extent of the DSCD measurements for 4 March 2005, calculated as the geometrical projection of the ozone maximum (18 km) for 86° (noon) and 91°. The blue and red lines indicate the geometrical projection of the ozone maximum at 91° for sunrise and sunset, respectively. The black line indicates the projection at 86°, which is the solar maximum on this day. The red star indicates the location of PEARL.

The NO_2 results, shown in Fig. 13b, do not display the same dramatic differences in the methods as the ozone results. Unlike the total ozone column, the NO_2 column has a diurnal cycle, and its concentrations are expected to vary throughout the twilight period. The 90° method takes this into account by finding the VCD at 90°, while the averaging method finds the average VCD between 86° and 91°. However, both methods assume that the same air mass is viewed throughout the twilight period, which is not the case in the first part of the campaign when Eureka was on the edge of the polar vortex. The fact that the two methods agree during the whole campaign is an indication that the NO_2 field is not as heterogeneous as the ozone field. The VCDs become less scattered after 8 March (day 67), when the vortex moves away from Eureka.

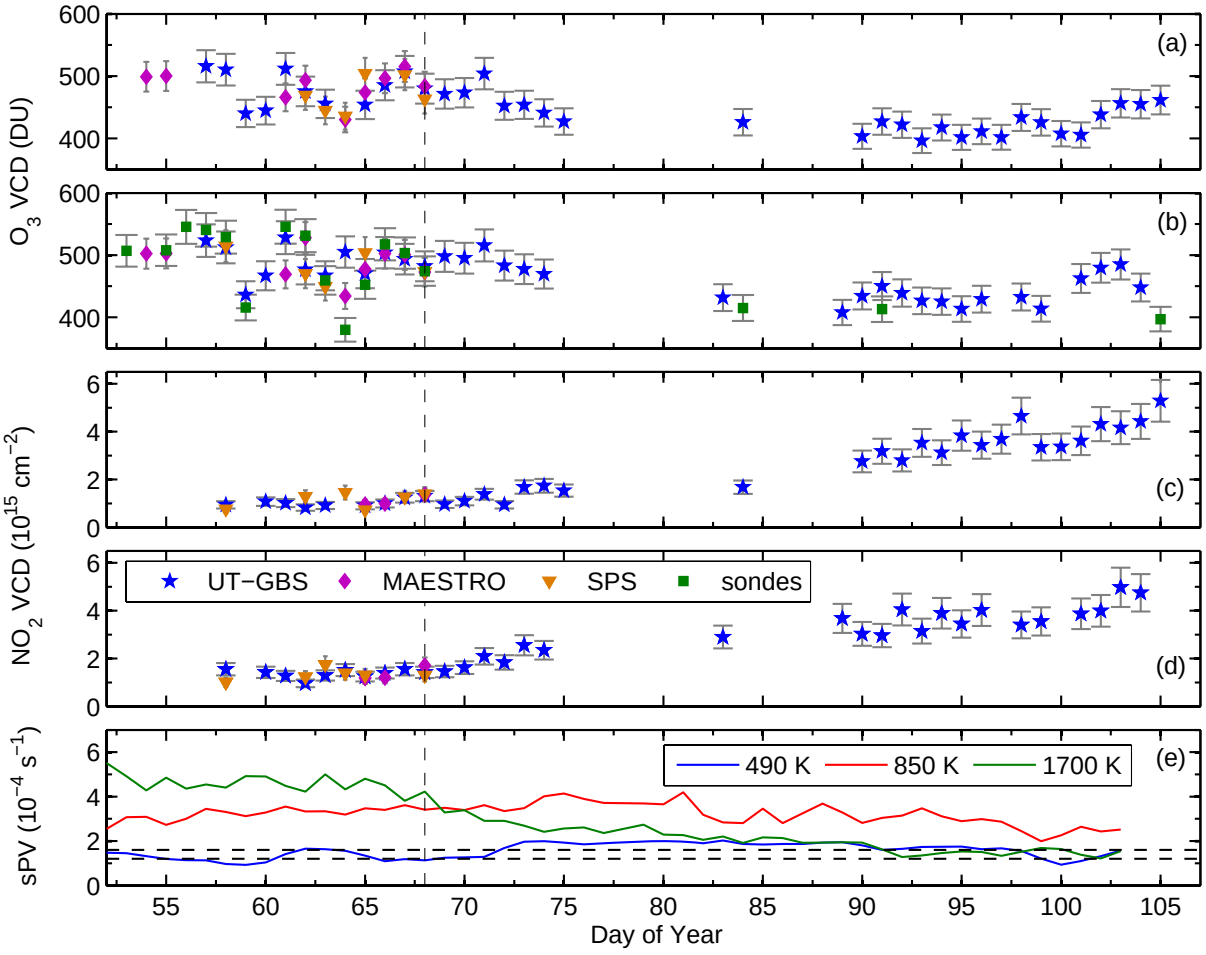

Fig. 15. Ozone **(a)** AM and **(b)** PM and NO_2 **(c)** AM and **(d)** PM vertical column densities from the campaign instruments and the ozonesondes for 2004. Error bars are the percentage errors given in Table 2. For the ozonesondes, the errors are ±5%. **(e)** The scaled potential vorticity calculated from GEOS-4 reanalysis for Eureka. The potential temperatures correspond to altitudes of ∽18 km, ∽30 km, and ∽50 km. The horizontal dashed lines indicate 1.2 and 1.6×10^{-4} s^{-1}, approximately demarking the edges of the polar vortex region. In all figures, the vertical dashed lines indicate the end of the intensive phase of the campaign.

6.2 Comparisons between ground-based instruments

6.2.1 2004

The ozone vertical column densities calculated using the averaging method from all the ground-based instruments for the Eureka 2004 campaign are shown in Fig. 15a and b. The averaging method is selected to minimise the morning and afternoon differences, due to the weighting towards noon, discussed in Sect. 6.1. In addition, Sarkissian et al. (1997) find the averaging method to better agree with ozonesondes. Also shown in Fig. 15b are integrated ozonesonde profiles. A correction has been added to the ozonesonde columns to account for ozone above the balloon burst height. Errors on the ozonesonde total columns are 5% (Tarasick et al., 2005).

In the following discussions, the average percentage difference is calculated using Eq. (2):

$$PD = 100 \times \sum_{i}^{n} \frac{\text{data}_{1,i} - \text{data}_{2,i}}{\text{average}_i} \quad (2)$$

PD is the percentage difference, data_1 and data_2 are the two data sets being compared, average is the average of the two data sets, *n* is the number of days of comparison, and *i* is the day index.

In Fig. 15a and b, the ozone VCDs of all three instruments (UT-GBS, SPS, and MAESTRO) agree within error bars on most days, and within an average of 0.7 DU (0.1%) to 10.7 DU (2.3%). During the entire campaign, the ozonesonde columns agree with the ground-based instruments within error on most days. The sonde columns agree within an average of 3.1 DU (0.2%) to 7.2 DU (2.0%) with

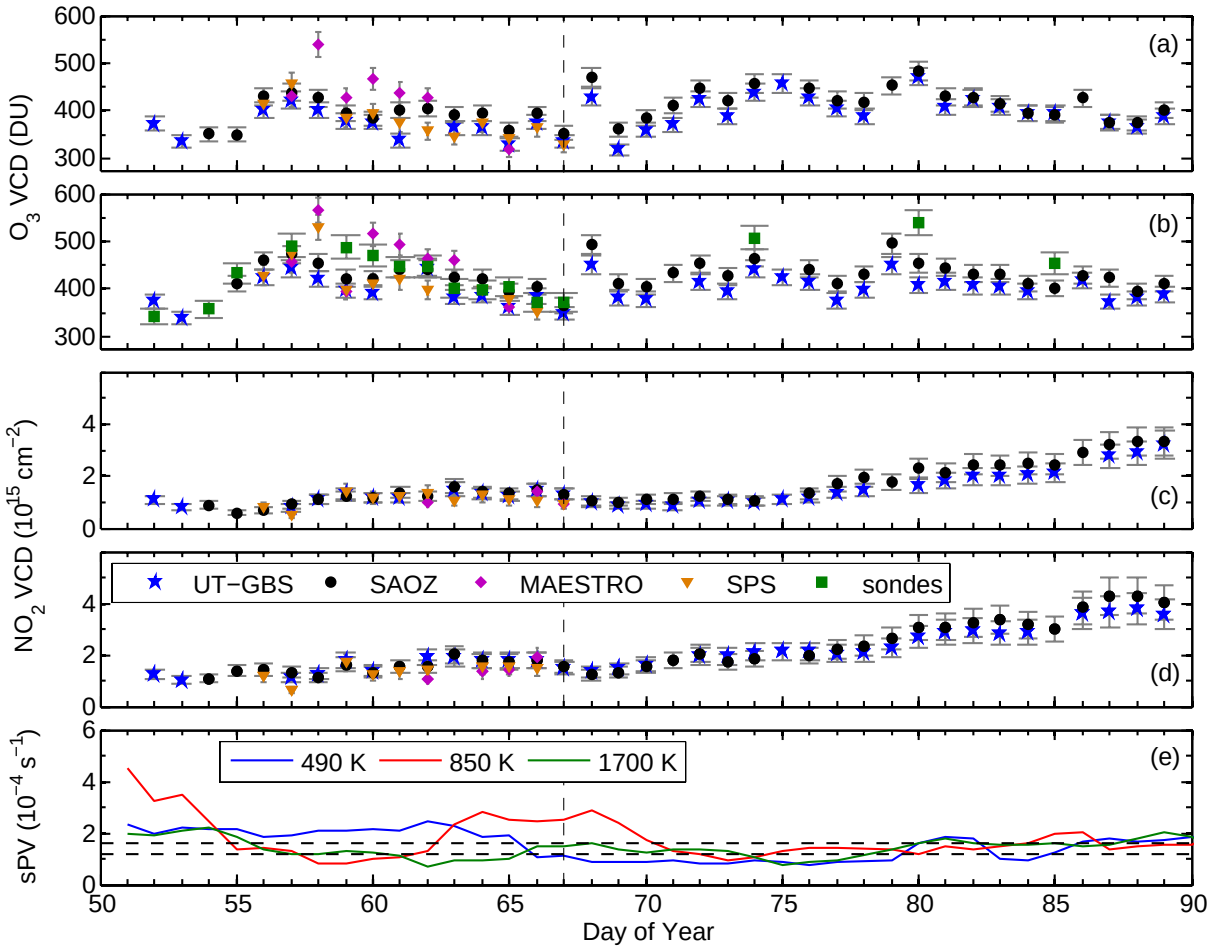

Fig. 16. Same as Fig. 15, but for 2005.

the ground-based columns and tend to be slightly higher. The campaign-averaged absolute and percentage differences for the ground-based instruments and the ozonesondes are given in Table 4. Also shown in this table is the combined percentage error in the VCDs from each pair of instruments compared. All the compared instruments agree within the combined errors.

The ground-based NO_2 VCDs found using the averaging method for the 2004 campaign are shown in Fig. 15c and d. The columns from the ground-based instruments generally agree within their combined error bars. The three instruments agree on average between 0.01×10^{14} molec/cm^2 (0.01%) and 1.4×10^{14} molec/cm^2 (8.5%). Table 4 gives the absolute and percentage differences for the ground-based instruments.

6.2.2 2005

Figure 16a and b show the morning and afternoon ozone VCDs from the ground-based instruments for the Eureka 2005 campaign. The columns from the UT-GBS, SAOZ, and SPS all mostly agree within error bars. The MAESTRO columns are larger than those from the other instruments, with the exception of day 65 (6 March). Generally, the MAESTRO columns do not agree with the other instruments within error bars. The UT-GBS, SAOZ, and SPS agree within 10.2 DU (2.6%) to 29.0 DU (5.8%), and these three instruments agree with MAESTRO within 29.6 DU (5.8%) to 62.6 DU (14.6%). The UT-GBS columns are the smallest of the four instruments.

The ozonesonde columns are higher than the ground-based columns, with the exception of MAESTRO, and mostly agree within error bars with SAOZ and the SPS. Half the individual comparisons with the UT-GBS, and two-thirds of the individual comparisons with MAESTRO do not agree within error bars. The sondes agree with the ground-based instruments between 0.47 DU (0.5%) and 38.9 DU (8.7%). Generally, the UT-GBS columns are the smallest of all the instruments. In Table 4, the individual comparisons agree within combined error, with the exception of the comparisons

Table 4. Campaign-averaged absolute and percentage differences (PDs) between the four ground-based instruments and the ozonesondes for ozone and NO_2 for the three Eureka campaigns. Ozone absolute differences are in DU, while NO_2 absolute differences are in 10^{14} molec/cm^2. Also shown is the combined percentage error for the two instruments that are compared (the sum in quadrature of the Table 2 errors for the relevant instruments.)

Comparison	Year	AM/PM	O_3 absolute (DU)	O_3 PD (%)	O_3 combined error (%)	NO_2 absolute (10^{14} molec/cm^2)	NO_2 PD (%)	NO_2 combined error (%)
SAOZ minus UT-GBS	2005	AM	20.7	5.3	5.8	2.08	12.3	23.2
		PM	29.0	6.9	5.8	1.03	2.2	23.2
	2006	AM	16.7	4.0	5.8	0.66	3.2	23.2
		PM	16.1	3.7	5.8	0.62	2.2	23.2
SPS minus UT-GBS	2004	AM	2.4	0.5	7.1	0.48	2.4	26.1
		PM	0.7	0.1	7.1	0.01	0.01	26.1
	2005	AM	10.2	2.6	6.5	−1.67	−16.3	25.9
		PM	12.6	2.6	6.5	−2.81	−20.8	25.9
	2006	AM	6.5	1.5	6.5	0.70	2.3	25.9
		PM	4.5	1.0	6.5	1.80	12.3	25.9
MAESTRO minus UT-GBS	2004	AM	2.6	0.6	6.9	0.32	2.9	26.1
		PM	−10.7	−2.3	6.9	−0.12	−0.4	26.1
	2005	AM	62.6	14.6	6.3	−1.98	−17.3	25.9
		PM	53.7	11.7	6.3	−3.72	−24.6	25.9
	2006	AM	14.5	3.3	6.3	−0.09	−4.5	25.9
		PM	2.3	0.5	6.3	−0.05	−1.8	25.9
SAOZ minus SPS	2005	AM	18.1	4.9	6.5	-1.87	-16.3	25.9
		PM	14.9	4.0	6.5	2.19	17.3	25.9
	2006	AM	13.9	3.3	6.5	−0.37	−0.3	25.9
		PM	−15.1	−3.5	6.5	−2.36	−16.3	25.9
SAOZ minus MAESTRO	2005	AM	-34.7	-7.4	6.3	2.08	18.6	25.9
		PM	−29.6	-5.8	6.3	2.70	18.9	25.9
	2006	AM	−7.2	−1.5	6.3	−0.16	−2.0	25.9
		PM	11.8	2.7	6.3	0.40	3.6	25.9
SPS minus MAESTRO	2004	AM	−4.4	−0.9	6.9	−0.90	−11.7	28.3
		PM	−10.3	-2.0	6.9	−1.40	−8.5	28.3
	2005	AM	−32.5	−7.8	6.9	−0.16	−1.0	28.3
		PM	−34.8	−7.4	6.9	0.52	5.5	28.3
	2006	AM	−13.1	−3.1	6.9	0.51	2.8	28.3
		PM	−2.6	−0.5	6.9	1.87	14.0	28.3
sondes minus UT-GBS	2004	PM	-7.2	-2.0	7.1			
	2005	PM	38.9	8.7	6.5			
	2006	PM	2.8	0.5	6.5			
sondes minus SAOZ	2005	PM	20.0	4.2	6.5			
	2006	PM	−11.9	−2.8	6.5			
sondes minus MAESTRO	2004	PM	3.1	0.2	6.9			
	2005	PM	0.47	0.5	6.9			
	2006	PM	−7.2	−1.7	6.9			
sondes minus SPS	2004	PM	6.9	1.3	7.1			
	2005	PM	35.6	8.3	7.1			
	2006	PM	−8.4	−2.0	7.1			

with MAESTRO, the SAOZ–UT-GBS afternoon, and the sondes–UT-GBS comparisons.

Figure 16c and d show the morning and afternoon NO_2 VCDs from the ground-based instruments. The UT-GBS, SAOZ, and SPS columns all agree within error bars on most days. The SAOZ columns tend to be larger than those of the other instruments. On average, the ground-based columns agree to within

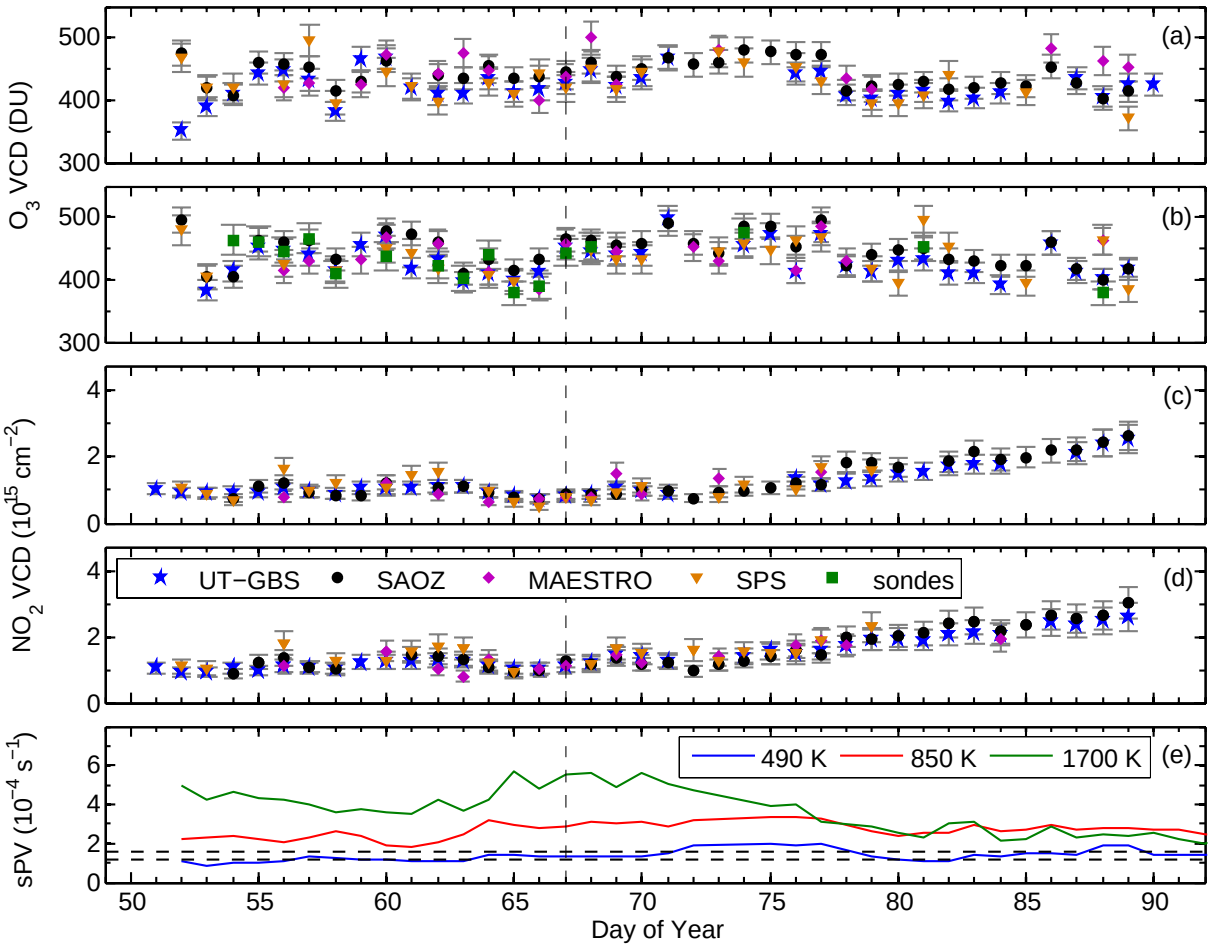

Fig. 17. Same as Fig. 15, but for 2006.

1.0×10^{14} molec/cm^2 (2.2%) to 3.7×10^{14} molec/cm^2 (24.6%).

6.2.3 2006

The morning and afternoon ozone VCDs for the Eureka 2006 campaign are shown in Fig. 17a and b. The ground-based instruments agree within error bars on most days. The MAESTRO and SPS columns are scattered about the SAOZ and UT-GBS columns, while the SAOZ columns are universally larger than those from the UT-GBS. On average, the instruments agree within 2.3 DU (0.5%) to 16.7 DU (4.0%). The agreement between the ozonesonde columns and the ground-based VCDs is also good, with the sonde columns being, on average, within 2.8 DU (0.5%) to 11.9 DU (2.8%). In Table 4, all the instrument comparisons agree within the combined percentage error.

The morning and afternoon NO_2 columns are shown in Fig. 17c and d. The UT-GBS and SAOZ are again in good agreement, with the SAOZ columns being larger than the UT-GBS columns. The SPS and MAESTRO are scattered about the UT-GBS and SAOZ columns. The columns are within 0.05×10^{14} molec/cm^2 (1.8%) to 2.4×10^{14} molec/cm^2 (16.3%) on average.

6.3 Comparisons with satellite instruments

6.3.1 2004

Integrated partial columns of ozone and NO_2 from the ACE-FTS and ACE-MAESTRO profiles taken within 500 km of Eureka are shown in Fig. 18, along with the average VCDs from the ground-based instruments. The partial columns were calculated by using the volume mixing ratio from the ACE-FTS and ACE-MAESTRO and the density from the ACE-FTS profiles. The ACE satellite overpasses are all in the afternoon, falling between 15:00 LT and 17:42 LT. All the overpasses correspond to SZAs of 89.5°. For ozone, the partial column is between 15 and 40 km. Kar et al. (2007) found these altitudes to be the region where ACE-MAESTRO data is appropriate for scientific analysis. The same altitude range is chosen for ACE-FTS to facilitate comparisons, especially

with ACE-MAESTRO. For the ACE-FTS, Dupuy et al. (2008) use a similar altitude region: 16–44 km. To account for the tropospheric ozone contribution below 15 km, the daily ozonesonde data below this altitude have been added to the satellite columns. The column below 15 km is between 98 DU and 207 DU, or about 30%. The ozonesondes launched during the three campaigns have total columns ranging between 350 DU and 560 DU. Assuming an exponential decay in the ozone column above the burst height of the balloon, the contribution to the total column from 40 to 100 km is between 1 DU and 16 DU. On average, the column above 40 km is 2% of the total column. Since the error on all the columns is greater than 2%, the ground-based total columns and satellite partial columns are expected to agree within error bars. A similar approach is used in Randall et al. (2002).

The average afternoon ozone VCDs from the three ground-based instruments are shown in Fig. 18a, along with the total columns from the ozonesondes and the partial columns from the satellite instruments. Only the period with satellite overpasses is shown. The ACE-FTS partial columns in Fig. 18a agree with the ground-based columns and sondes for most days. On average, the ACE-FTS partial columns agree with the four sets of ground-based and sonde VCDs within 9.0 DU (1.8%) to 30.8 DU (6.1%) (see column 4 of Table 5). The ACE-MAESTRO partial columns are generally smaller than those from the ground-based instruments and sondes, and for the most part do not agree within error bars. On average, the ACE-MAESTRO partial columns agree within 53.8 DU (12.3%) to 88.5 DU (20.1%) with the ground-based and sonde columns. The ACE-FTS partial columns are larger than those of the ACE-MAESTRO, with the exception of days 55 and 70. The ACE-FTS columns are an average of 100.9 DU (22.5%) larger than the ACE-MAESTRO columns. The absolute and percentage differences for the individual instrument comparisons with the satellite instruments are shown in Table 5, as well as the combined percentage error of each pair of instruments compared. For comparisons with ACE-FTS, all of the individual comparisons agree within the combined error of the two instruments. For comparisons with ACE-MAESTRO, the individual comparisons do not agree within the combined error of the two instruments.

The altitude range recommended by Kar et al. (2007) for ACE-MAESTRO is used for the NO_2 partial columns: 22 to 40 km. The same region is used for both ACE-FTS and ACE-MAESTRO. Kerzenmacher et al. (2008) use a larger region for the ACE-FTS: 13–58 km. No correction is made to the NO_2 satellite partial columns to account for the NO_2 below 22 km and above 40 km. To quantify the contribution of the column above and below the partial column, NO_2 profiles for late February and early March at 80° N have been generated by the University of California, Irvine (UCI) photochemical box model (Prather, 1997; McLinden et al., 2000). The total column of NO_2 during this time is between 1.29×10^{14} molec/cm^2 and 8.51×10^{14} molec/cm^2, with the column steadily increasing over the time period. The contribution below 22 km is 0.09×10^{14} molec/cm^2 (7.34%) in mid-February and 1.04×10^{14} molec/cm^2 (12.22%) in mid-March. The NO_2 below 22 km is steadily increasing over the time period. The contribution from above 40 km is 0.11×10^{14} molec/cm^2 (7.20%) in mid-February and 0.09×10^{14} molec/cm^2 (1.03%) in mid-March. The NO_2 above 40 km is steadily decreasing over the time period. The total contribution from these two regions is between 12.4% and 14.6%. As a result, the satellite partial columns are expected to be roughly 13% smaller than the ground-based total columns.

The average afternoon columns of NO_2 from the ground-based instruments and the partial columns from the satellite instruments are shown in Fig. 18b. Table 5 gives the absolute and percentage differences between the satellite and ground-based instruments. Both the ACE-FTS and ACE-MAESTRO partial column measurements follow the general trend of the ground-based total column measurements and agree within error bars. The ACE-FTS partial columns are within an average of 0.6×10^{14} molec/cm^2 (3.3%) to 1.8×10^{14} molec/cm^2 (13.9%) of the ground-based instruments. The ACE-MAESTRO columns are within an average of 0.2×10^{14} molec/cm^2 (0.1%) to 0.9×10^{14} molec/cm^2 (6.4%) of the ground-based instruments. The ACE-FTS and ACE-MAESTRO partial columns generally agree within error bars, with the ACE-FTS columns being 2.0×10^{14} molec/cm^2 (17.1%) smaller than the ACE-MAESTRO columns. The difference between the ACE-FTS and the UT-GBS and SPS total columns is approximately the expected percent difference, given the expected vertical distribution of NO_2.

6.3.2 2005

The average afternoon ozone VCDs from the ground-based instruments are shown in Fig. 19a, along with the total columns from the ozonesondes, and the partial columns from the satellite instruments. The ACE-FTS partial columns agree with the ground-based instruments and the sondes on most days of the campaign. On average, the ACE-FTS columns agree with the ground-based instruments and ozonesondes within 1.5 DU (0.1%) to 27.2 DU (6.3%). The agreement between the ACE-MAESTRO and the other instruments is improved this year. On average, the ACE-MAESTRO partial columns agree with the UT-GBS, SAOZ, SPS, and ozonesondes between 4.7 DU (2.6%) and 45.7 DU (12.6%), and with the MAESTRO within 84.4 DU (20.6%). The ACE-FTS columns are 26.6 DU (7.8%) larger than the ACE-MAESTRO columns. In Table 5, all the comparisons with ACE-FTS are within the combined percentage error of the individual instruments. The comparisons with ACE-MAESTRO are generally not within the combined percentage error.

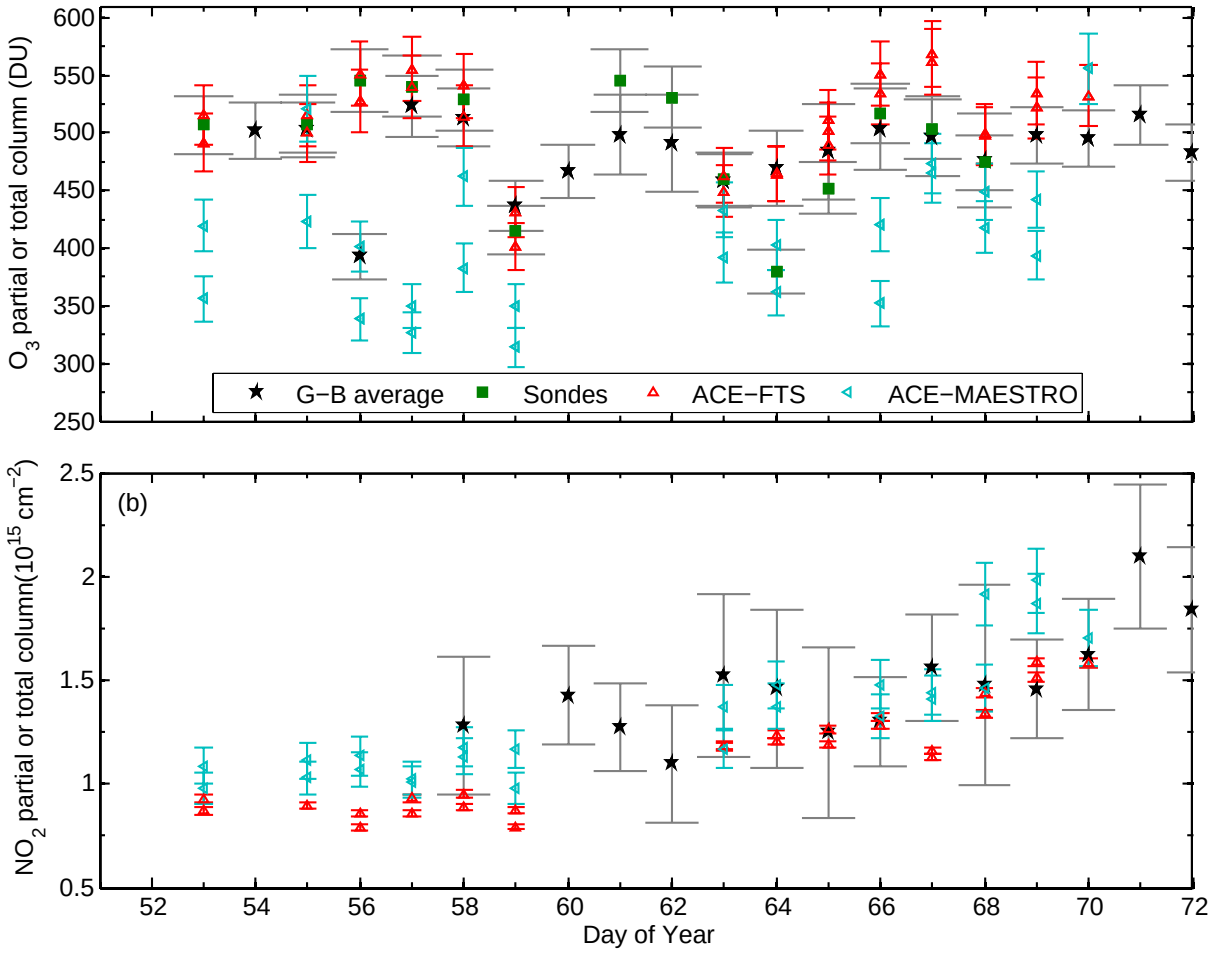

Fig. 18. Afternoon **(a)** ozone and **(b)** NO_2 vertical column densities from the campaign instruments, ozonesondes, and partial columns from ACE-FTS, and ACE-MAESTRO for 2004. For both species, the ground-based measurements have been averaged. Error bars for the ground-based VCDs are the sum in quadrature of the relevant percentage errors given in Table 2. For the ozonesondes, the errors are 5%. For ACE-FTS, the error bars represent only spectral fitting error, while for the ACE-MAESTRO the error bars are a combination of fitting error, errors in the cross-sections, and errors arising from unaccounted-for temperature effects in the cross-sections. For the satellite measurements, the partial columns are taken between 0 and 40 km for ozone and between 22 and 40 km for NO_2.

Figure 19b shows the average total NO_2 columns from the ground-based instruments and the partial columns from the satellite instruments. As in 2004, the ACE-FTS and ACE-MAESTRO partial columns follow the trend of the ground-based instruments and agree with these instruments within error bars. The ACE-FTS partial columns are within 0.12×10^{14} molec/cm^2 (0.8%) to 1.8×10^{14} molec/cm^2 (11.9%) of the ground-based total columns. The ACE-MAESTRO columns agree with the ground-based instruments within 0.8×10^{14} molec/cm^2 (5.5%) to 1.2×10^{14} molec/cm^2 (7.9%). The ACE-FTS and ACE-MAESTRO columns are again in good agreement, with the ACE-FTS columns 0.8×10^{14} molec/cm^2 (5.7%) smaller than the ACE-MAESTRO columns.

The ACE-FTS partial columns and the UT-GBS and SAOZ total columns differ by the expected percentage difference.

6.3.3 2006

The average total ozone columns from the ground-based instruments, the total columns from the ozonesondes, and the partial columns from the satellite instruments, are shown in Fig. 20a. As in 2004 and 2005, the ACE-FTS partial columns mostly agree within error bars with the total columns from the ground-based instruments and the ozonesondes. The agreement is, on average, between 19.5 DU (4.3%) and 38.9 DU (9.0%). There is again an improvement in the comparison of the ACE-MAESTRO columns with the other

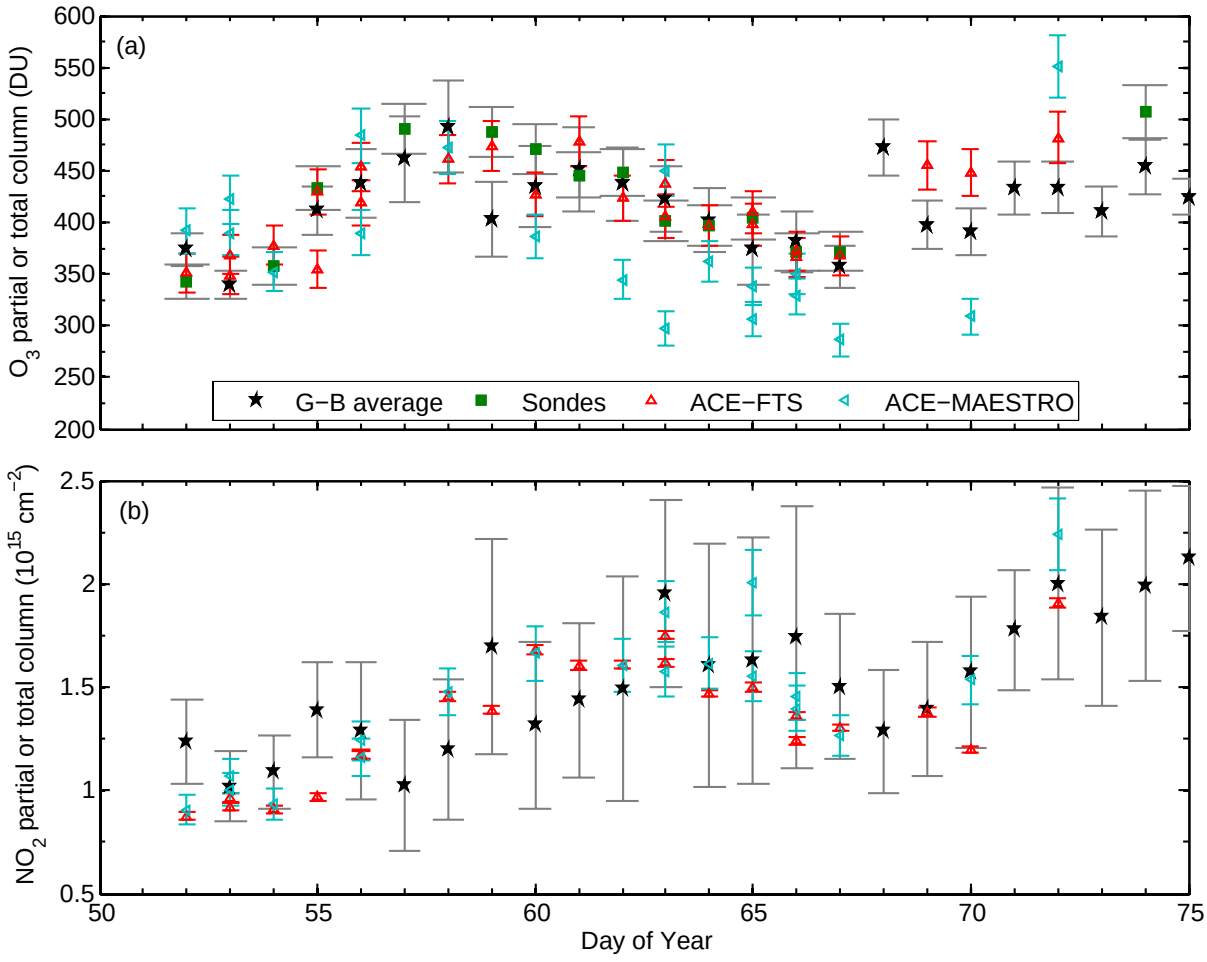

Fig. 19. Same as Fig. 18, but for 2005.

instruments. The satellite partial columns are within 4.4 DU (1.2%) to 7.5 DU (2.2%) of the ground-based instruments and the ozonesondes. The ACE-FTS and ACE-MAESTRO columns are within 23.4 DU (5.5%) of each other.

The average total NO_2 columns from the ground-based instruments and the satellite partial columns are shown in Fig. 20b. As in the other campaigns, the ACE-FTS and ACE-MAESTRO partial columns follow the same general trend as the ground-based instruments. The ACE-FTS partial columns are within 1.4×10^{14} molec/cm^2 (13.6%) to 2.9×10^{14} molec/cm^2 (27.2%) of the four sets of ground-based total columns. The ACE-MAESTRO columns are within 1.1×10^{14} molec/cm^2 (9.8%) to 3.2×10^{14} molec/cm^2 (27.4%) of the ground-based columns. The ACE-FTS columns are 3.9×10^{14} molec/cm^2 (35.0%) smaller than the ACE-MAESTRO columns. The ACE-FTS partial columns are smaller than the SAOZ total columns by the expected percentage difference.

6.4 Summary of satellite comparisons

Figure 21a–d shows scatter plots of the ACE-FTS and ACE-MAESTRO partial columns versus the ground-based and ozonesonde total columns for both species. Also shown are the linear fits to the ensembles of data points. For ozone, the expected slope is one and the expected intercept is zero. For NO_2, the expected slope is one and the expected intercept is on the order of -10^{14} molec/cm^2, which accounts for the difference between the total and partial columns compared. The ACE-FTS vs. ground-based instrument scatter plots for ozone (Fig. 21a) and NO_2 (Fig. 21b) are compact, with the data scattered evenly about the fitted line. Both slopes are close to one, and include one within the calculated error of the slope. The ozone intercept is small, while the NO_2 intercept is of the expected order of magnitude. This reflects the good agreement seen in Table 5.

The ACE-MAESTRO versus ground-based instrument scatter plots for ozone (Fig. 21c) and NO_2 (Fig. 21d) show significantly more scatter than the ACE-FTS comparisons.

Table 5. Campaign-averaged absolute and percentage differences (PDs) between the ACE-FTS and ACE-MAESTRO and the four ground-based instruments and the ozonesondes for ozone and NO_2 for the three Eureka campaigns. Ozone absolute differences are in DU, while NO_2 absolute differences are in 10^{14} molec/cm^2. The combined percentage error for the two compared instruments is also given, and is the sum in quadrature of the individual percentage errors. "G-B avg." is the average column from the ground-based instruments.

Comparison	Year	O_3 absolute (DU)	O_3 PD (%)	O_3 combined error (%)	NO_2 absolute (10^{14} molec/cm^2)	NO_2 PD (%)	NO_2 combined error (%)
ACE-FTS minus G-B avg	2004	28.3	5.6	9.9	−1.62	−12.8	32.9
	2005	9.8	2.3	10.4	−1.40	-10.5	36.6
	2006	27.8	6.2	10.4	−2.00	−20.0	36.6
ACE-FTS minus UT-GBS	2004	17.3	3.2	7.1	−1.80	−13.9	16.9
	2005	27.2	6.3	6.5	−1.59	−10.7	16.5
	2006	27.6	6.3	6.5	−1.93	−19.7	16.5
ACE-FTS minus SAOZ	2005	1.5	0.1	6.5	−1.75	−11.9	16.5
	2006	19.5	4.3	6.5	−1.39	−13.6	16.5
ACE-FTS minus MAESTRO	2004	30.8	6.1	6.7	−0.61	−3.3	20.1
	2005	−17.8	-3.1	7.0	−0.98	−4.6	20.1
	2006	31.8	7.2	7.0	−2.94	−27.2	20.1
ACE-FTS minus SPS	2004	9.0	1.8	7.1	−1.66	−12.3	20.1
	2005	17.4	4.4	7.1	0.12	0.78	20.1
	2006	38.9	9.0	7.1	−2.80	−24.2	20.1
ACE-FTS minus sondes	2004	21.0	4.4	7.1			
	2005	−4.4	−1.0	7.1			
	2006	20.0	4.7	7.1			
ACE-MAESTRO minus G-B avg	2004	−69.9	−16.4	10.2	0.36	1.3	34.5
	2005	−20.6	−6.4	10.6	−0.37	−3.3	37.4
	2006	−1.6	−0.6	10.6	2.00	16.7	37.4
ACE-MAESTRO minus UT-GBS	2004	−83.8	−19.4	7.4	0.18	−0.1	19.7
	2005	−4.7	−2.6	6.8	−0.84	−5.8	18.2
	2006	−4.4	−1.2	6.9	1.91	15.6	18.2
ACE-MAESTRO minus SAOZ	2005	−45.1	−12.9	6.8	−0.81	−5.5	18.2
	2006	−7.1	−1.9	6.9	3.21	27.4	18.2
ACE-MAESTRO minus MAESTRO	2004	-53.8	-12.3	7.3	0.88	6.4	22.5
	2005	-84.4	−20.6	7.3	0.86	6.7	21.5
	2006	5.0	1.1	7.3	1.05	9.8	21.5
ACE-MAESTRO minus SPS	2004	-56.3	−12.5	7.4	0.19	1.9	22.5
	2005	−29.2	−7.9	7.4	1.24	7.9	21.5
	2006	-7.5	−2.2	7.4	1.51	13.5	21.5
ACE-MAESTRO minus sondes	2004	−88.5	-20.1	7.4			
	2005	−45.7	−12.6	7.4			
	2006	6.2	1.4	7.4			
ACE-FTS minus ACE-MAESTRO	2004	100.9	22.5	7.5	−2.06	−17.1	10.4
	2005	26.6	7.8	7.5	−0.80	−5.7	8.0
	2006	23.4	5.5	7.5	−3.92	−35.0	8.1

Neither slope is close to unity. This reflects the larger scatter in the ACE-MAESTRO partial columns compared to the ground-based instruments. The ozone intercept is large, while the NO_2 intercept is of the expected order of magnitude, but is of the wrong sign. This reflects the large differences seen in Table 5.

Figure 21e and f show the scatter plots for ACE-FTS versus ACE-MAESTRO for ozone and NO_2. In this case, the expected slope is one and the expected intercept is zero for both species. For ozone, the slope is not close to unity, and

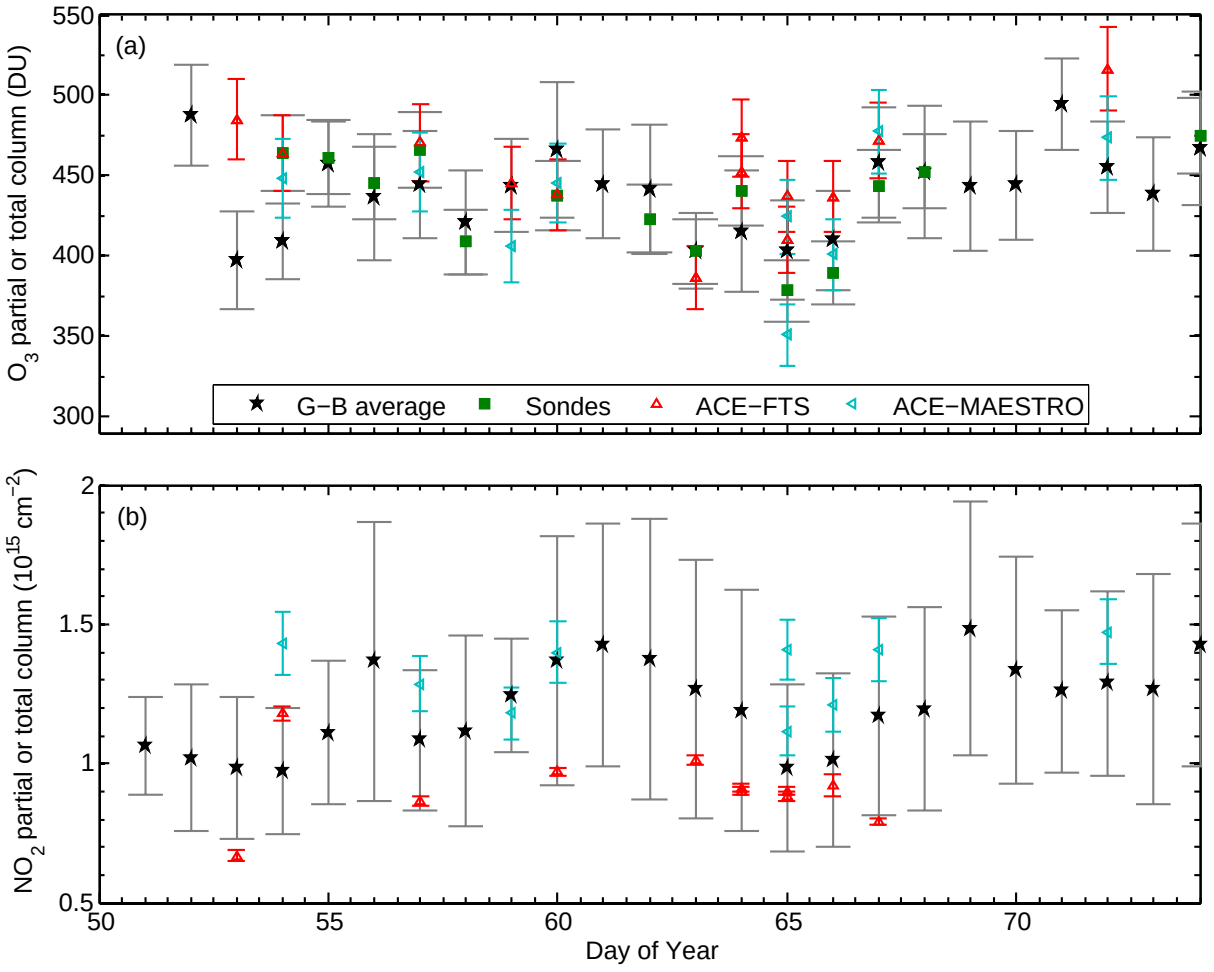

Fig. 20. Same as Fig. 18, but for 2006.

the intercept is large. This reflects the large differences between the instruments seen in Table 5. For NO_2, the slope is close to unity, although the intercept is large. The scatter plot is also compact. This indicates that the instruments agree in the overall trends in NO_2, but differ in the values of the partial columns. This is again indicative of the large differences seen in Table 5.

7 Consideration of meteorological conditions

Figures 15e, 16e, and 17e show the scaled potential vorticity (sPV) calculated from GEOS-4 reanalysis data for sunrise (SZA=90°) at Eureka (Bloom et al., 2005; Manney et al., 1994). A description of how the sPV is calculated is given in Manney et al. (2007b). sPV is shown on three potential temperature levels: 490 K (∽18 km, lower stratosphere), 850 K (∽30 km, middle stratosphere), and 1700 K (∽50 km, upper stratosphere). The values for sunset have also been calculated, and are similar to the sunrise values. To first order, sPV values below 1.2×10^{-4} s^{-1} indicate that Eureka is outside the vortex, while those above 1.6×10^{-4} s^{-1} indicate that Eureka is inside the vortex. Values that fall in between indicate that Eureka is on the edge of the vortex (Manney et al., 2007a).

7.1 2004

In 2004 the polar vortex had reformed over Eureka in the middle and upper stratosphere, with a weak vortex in the lower stratosphere. As can be seen in Fig. 15e, through most of the campaign, Eureka was well inside the vortex at higher altitudes. In the lower stratosphere, where the peak in ozone is found (∽15–20 km), Eureka is on the edge or outside the vortex until day 62 (2 March), when it briefly enters the vortex until day 65 (5 March). It then returns to the edge of the vortex until day 72 (12 March), where it stays until day 99 (9 April). On day 102 (11 April) it enters the vortex again. Most of the instruments see a drop in ozone as Eureka enters the vortex on day 62, and then a return to the levels seen earlier in

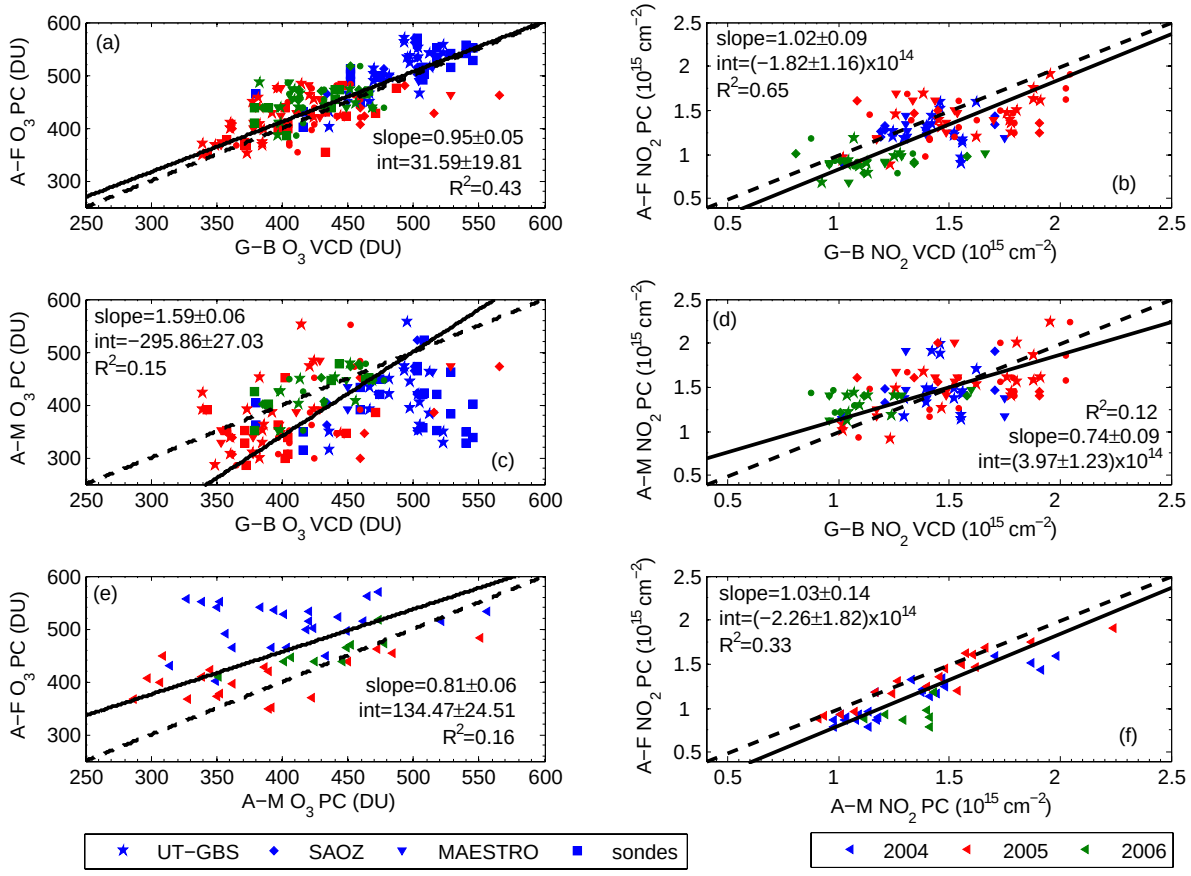

Fig. 21. Scatter plot of **(a)** ACE-FTS (A-F) ozone partial columns (PC) vs. ground-based (G-B) total columns and total columns from the ozonesondes. **(b)** Same as (a), but for NO_2. **(c–d)** Same as (a–b), but for ACE-MAESTRO (A-M) partial columns. **(e–f)** Same as (a–b) but for ACE-FTS vs. ACE-MAESTRO. In all figures, the solid line shows the fitted relationship between the two data sets being compared. The slope, intercept, and R^2 for the comparisons are given on the figure. The dotted line shows the one-to-one line relationship for comparison. The blue points are for 2004, the red points are for 2005, and the green points are for 2006. The satellite partial columns are between 0 and 40 km for ozone and between 22 and 40 km for NO_2.

the campaign on day 65. The ozone remains fairly constant until day 72, when it begins to decrease as Eureka enters the vortex again. The ozone then levels off at the end of March, remaining so until day 99, when it begins to decrease. On day 102 (11 April) the ozone shows a slight recovery as the vortex moves over Eureka once again.

The behaviour of NO_2 during the campaign is dominated by the recovery of NO_2 after the polar night, with the reservoir species N_2O_5 being photolysed. Morning and afternoon columns begin to agree towards the end of the campaign as the Sun is continuously above the horizon after 14 April (day 105). The peak in the NO_2 profile is between 25 and 35 km, with large contributions in the lower stratosphere as well. In the middle stratosphere, Eureka is inside the vortex until day 92 (1 April), and remains on the edge of the vortex until the end of the campaign. The NO_2 and ozone columns are inversely related during the campaign. NO_2 is steadily increasing, with larger values from day 62–65. As the ozone decreases after day 72, the NO_2 steadily increases. At the end of the campaign, when the middle stratosphere is on the edge of the vortex, the two species appear to be positively correlated. When ozone decreases beginning day 99, NO_2 decreases as well.

7.2 2005

In 2005, Eureka was on the edge or outside of the vortex until 8 March (day 67), when the vortex moved away from Eureka and began to break apart. From Fig. 16e, the lower stratosphere was inside the vortex until day 65 (6 March), on the edge until day 67 (March 8), and then outside the vortex for the remainder of the campaign. The remnants of the vortex returned for two brief periods: day 80–82 (21–23 March) and day 86–91 (27 March–1 April). Until day 65, all of the instruments observe a decreasing ozone column.

As the vortex moves away, the ozone concentrations begin to stabilise and increase, then begin to decrease again after day 75 (16 March). There is a slight increase as the vortex moves back to Eureka on day 80, and then the column decreases until the end of the campaign.

In the middle stratosphere, Eureka is inside the vortex until day 56 (25 February), and then outside or on the edge until day 80, when it enters the vortex. On day 88 (29 March), the vortex moves away from Eureka again. The NO_2 columns increase until day 65, when they show a slight decrease, recovering by day 68, when they increase until day 82, when the columns begin to decrease again. On day 86 they have recovered and keep increasing until the end of the campaign. Until day 65, and after day 82, the NO_2 and ozone columns are inversely related. In between these days, both the ozone and NO_2 columns are generally increasing.

7.3 2006

From Fig. 17, the upper and middle stratosphere were inside the vortex for the entire campaign. The vortex in the lower stratosphere did not reform substantially after the sudden stratospheric warming in January. The ozone field observed by all of the instruments is relatively constant throughout the campaign.

In the middle stratosphere, the sPV increases sharply on day 63 (2 March), and remains high until day 77 (18 March), indicating that Eureka moves further into the vortex at these altitudes. The NO_2 columns increase until day 63, when they start to decrease slightly. The columns continue to vary inversely with the sPV until day 77, when they increase uniformly until the end of the campaign.

8 Conclusions

The ozone and NO_2 DSCDs and VCDs from four UV-visible zenith-sky instruments have been compared following the techniques adopted by the UV-visible Working Group of the NDACC. The ozone DSCDs Type 1 comparisons are found to partially meet the NDACC standards: approximately 60% of the slopes meet the standard. Those comparisons that do not meet the standard are within the standard error, with the exception of comparisons with a small number (less than ten) of twilight periods to compare, the UT-GBS vs. SAOZ comparisons in 2005, and the SPS vs. SAOZ afternoon comparison in 2006. These comparisons are thought to disagree due to the different fields-of-view of the instruments, as well as Eureka's position on the edge of the polar vortex in 2005. While the comparisons that meet the standards within the standard error (which represents the random error) fail to meet the NDACC standards, their range of possible values includes part of the NDACC range. Not meeting the NDACC standards within the standard error implies that there is a systematic bias between the instruments. The residuals are generally larger than the standards, indicating scatter in the DSCDs. The ozone Type 2 comparisons are also found to partially agree with the NDACC standards, with the ratios mostly meeting the requirements in 2006, but the standard deviations being larger than the requirement.

The NO_2 Type 1 comparisons also partially meet the NDACC standards. The UT-GBS vs. SAOZ comparisons meet all three standards in 2006, and all but one in 2005. About 60% of the slopes meet the NDACC standards. The intercepts meet the NDACC standards, with large standard errors. The residuals are much larger than the standards. The Type 2 comparisons for NO_2 are better, with most of the ratios meeting the NDACC standards. The standard deviations are large, which could be a result of the small NO_2 columns in the polar springtime.

These comparisons are generally an improvement over comparisons between the same instruments during the MANTRA 2004 campaign (Fraser et al., 2007).

Two methods of finding the vertical column density of ozone from the slant column densities were compared. The averaging method and Langley plot method are found to produce similar results when observing homogenous trace gas fields. When the fields are not homogenous, such as the case during the beginning of the Eureka 2005 campaign, the results can be very different.

For ozone, in all the campaigns, the ground-based instruments, ozonesondes, and satellite instruments generally agree within the combined error bars of the instruments. The ground-based instruments agree within 62.6 DU (14.6%) for all campaigns. For all but six of the 30 possible instrument pair comparisons, the average difference between the ground-based VCDs is less than the combined error bars of the instruments. The six comparisons that do not agree are all from 2005, when Eureka was on the edge of the polar vortex, which has the greatest horizontal gradient in the ozone field. The ozonesondes and the ground-based instruments agree within 38.9 DU (8.7%) for all campaigns. Generally, the sonde columns fall within the range of VCDs from the ground-based instruments. Nine of the eleven ground-based instrument vs. sonde comparisons agree within the combined error bars of the instruments. The two comparisons that fall outside this range are from 2005.

For the ACE-FTS, 12 of the 14 comparisons to the ground-based instruments and ozonesondes agree within the combined error bars of the instruments. For the ACE-MAESTRO, only 5 of the 14 comparisons agree to within the combined error bars of the instruments.

For NO_2, during all the campaigns, the ground-based data mostly agree within error bars. The four instruments agree within 3.7×10^{14} molec/cm^2 (24.6%) for all the campaigns. All of the 30 possible instrument pair comparisons agree to within the combined error bars of the instruments. Both the ACE-FTS and ACE-MAESTRO partial columns follow the trend in NO_2 VCD as seen by the ground-based instruments. The NO_2 partial columns from the satellite instruments are

Table 6. Average differences between the satellite instruments and the average of the ground-based instruments and, in the case of ozone, ozonesondes (G-B avg.). Also shown is the average difference between ACE-FTS and ACE-MAESTRO. For the ground-based instruments and the ozonesondes these are total vertical columns. For the satellite instruments these are partial columns: between 0 and 40 km for ozone and between 22 and 40 km for NO_2.

Comparison	O_3	NO_2
ACE-FTS minus G-B avg.	4.5%	−13.4%
ACE-MAESTRO minus G-B avg.	−9.9%	2.5%
ACE-FTS minus ACE-MAESTRO	14.4%	−15.5%

expected to be roughly 13% smaller than the total columns from the ground-based instruments.

The average differences between the satellite instruments and the average of the ground-based instruments and, in the case of ozone, ozonesondes is given in Table 6. The ACE-FTS ozone partial columns agree within the combined error bars of the total columns from the ground-based instruments, while the NO_2 partial columns differ from the total columns from the ground-based instruments by the expected percentage. The ACE-MAESTRO ozone partial columns are smaller than the total columns from the ground-based instruments, while the NO_2 partial columns are larger than those of the ground-based instruments. For ozone, these results are consistent with Dupuy et al. (2008), who found that profiles and partial columns from satellite-, aircraft-, balloon-, and ground-based instruments agree to within ±10% (generally +5%) of the ACE-FTS measurements, and to within ±10% (generally better than ±5%) of the ACE-MAESTRO measurements. For NO_2, these results are consistent with Kerzenmacher et al. (2008), who found that partial columns from five ground-based Fourier transform infrared spectrometers agree to within 10.1% of the ACE-FTS partial columns and to within 17.6% of the ACE-MAESTRO partial columns.

Table 6 also shows the average difference between ACE-FTS and ACE-MAESTRO. For ozone, the partial columns from the ACE-FTS are 14.4% larger than those from ACE-MAESTRO. For NO_2, the partial columns from the ACE-FTS are 15.5% smaller than those from the ACE-MAESTRO. The agreement between the two satellite instruments varies significantly between the different years.

Acknowledgements. The Canadian Arctic ACE Validation campaign project has been supported by the Canadian Space Agency (CSA), Environment Canada (EC), the Natural Sciences and Engineering Research Council (NSERC) of Canada, the Northern Scientific Training Program and the Centre for Global Change Science at the University of Toronto. Logistical and on-site technical support for the 2006 campaign was provided by the Canadian Network for the Detection of Atmospheric Change (CANDAC). CANDAC and PEARL are funded by the Canadian Foundation for Climate and Atmospheric Sciences (CFCAS), NSERC, the Canadian Foundation for Innovation, the Ontario Innovation Trust, the Ontario Ministry of Research and Innovation, and the Nova Scotia Research and Innovation Trust. The SAOZ participation in the campaigns was supported by the Centre National D'Études Spatiales. The Atmospheric Chemistry Experiment (ACE), also known as SCISAT-1, is a Canadian-led mission mainly supported by the CSA and NSERC. The MAESTRO instrument was developed with additional financial support from EC, CFCAS, and NSERC.

WinDOAS was provided by C. Fayt and M. Van Roozendael of the Belgian Institute for Space Aeronomy (IASB-BIRA).

Work at the Jet Propulsion Laboratory, California Institute of Technology, was done under contract with the National Aeronautics and Space Administration.

PV plots were downloaded from the webpage http://www.pa.op.dlr.de/arctic. The ECMWF data used for generating the plots were available through the special project "Effect of non-hydrostatic gravity waves on the stratosphere above Scandinavia" by A. Dörnbrack.

The calculation of the location of the slant column measurements in Fig. 14 was performed by Dmitry Ionov of the Research Institute of Physics, St. Petersburg, Russia.

Thanks to the staff of the Eureka weather station for the ozonesonde launches and their hospitality during the campaigns.

The authors also thank Howard Roscoe and an anonymous reviewer for their comments which improved this manuscript.

Edited by: T. Wagner

References

Bassford, M. R., Strong, K., McLinden, C. A., and McElroy, C. T., Ground-based measurements of ozone and NO_2 during MANTRA 1998 using a zenith-sky spectrometer, Atmos.-Ocean, 43, 325–338, 2005.

Bernath, P. F., McElroy, C. T., Abrams, M. C., et al.: Atmospheric Chemistry Experiment (ACE): mission overview, Geophys. Res. Lett., 32, L15S01, doi:10.1029/2005GL022386, 2005.

Bloom, S. C., da Silva, A., Dee, D., et al.: The Goddard Earth Observing Data Assimilation System, GEOS DAS Version 4.0.3: Documentation and Validation, Tech. Rep. 104606 V26, NASA, 2005.

Boone, C. D., Nassar, R., Walker, K. A., Rochon, Y., McLeod, S. D., Rinsland, C. P., and Bernath, P. F.: Retrievals for the Atmospheric Chemistry Experiment Fourier-Transform Spectrometer, Appl. Optics, 44, 7218–7231, 2005.

Burrows, J. P., Richter, A., Dehn, A., Deters, B., Himmelmann, S., Voight, S., and Orphal, J.: Atmospheric remote-sensing reference data from GOME – 2. Temperature dependent absorption cross-sections of O_3 in the 231–794 nm range, J. Quant. Spectrosc. Radiat. Transfer, 61, 509–517, 1999.

Chance, K. V. and Spurr, R. J. D.: Ring effect studies: Rayleigh scattering, including molecular parameters for rotational Raman scattering, and the Fraunhofer spectrum, Appl. Optics, 36, 5224–5230, 1997.

Dupuy, E., Walker, K. A., Kar, J., et al.: Validation of ozone measurements from the Atmospheric Chemistry Experiment (ACE),

Atmos. Chem. Phys. Discuss., 8, 2513–2656, 2008, http://www.atmos-chem-phys-discuss.net/8/2513/2008/.

Farahani, E.: Stratospheric composition measurements in the Arctic and at mid-latitudes and comparison with chemical fields from atmospheric models, Ph.D. Thesis, University of Toronto, Toronto, 2006.

Fayt, C. and Van Roozendael, M.: WinDOAS 2.1 – Software user manual, Uccle, Belgium, BIRA-IASB, 2001.

Fraser, A., Bernath, P. F., Blatherwick, R. D., et al.: Intercomparison of ground-based ozone and NO_2 measurements during the MANTRA 2004 campaign, Atmos. Chem. Phys., 7, 5489–4599, 2007, http://www.atmos-chem-phys.net/7/5489/2007/.

Greenblatt, G. F., Orlando, J. J., Burkholder, J. B., and Ravishankara, A. R.: Absorption measurements of oxygen between 330 and 1140 nm, J. Geophys. Res., 95, 18 577–18 582, 1990.

Hofmann, D. J., Bonasoni, P., De Mazière, M., et al.: Intercomparison of UV/visible spectrometers for measurements of stratospheric NO_2 for the Network for the Detection of Stratospheric Change, J. Geophys. Res., 100, 16 765–16 791, 1995.

Johnston, P. V., Pommereau, J.-P., and Roscoe, H. K.: Appendix II – UV/Vis instruments, http://www.ndacc.org/, 1999.

Kar, J., McElroy, C. T., Drummond, J. R., et al.: Initial comparison of ozone and NO_2 profiles from ACE-MAESTRO with balloon and satellite data, J. Geophys. Res., 112, D16301, doi:10.1029/2006JD008242, 2007.

Kerzenmacher, T. E., Walker, K. A., Strong, K., et al.: Measurements of O_3, NO_2 and temperature during the 2004 Canadian Arctic ACE Validation Campaign, Geophys. Res. Lett., 32, L16S07, doi:10.1029/2005GL023032, 2005.

Kerzenmacher, T. E., Wolff, M., Strong, K., et al.: Validation of NO and NO_2 from ACE-FTS and MAESTRO, Atmosp. Chem. Phys. Discuss., 8, 3027–3142, 2008.

Kurylo, M. J. and Zander, R. J.: The NDSC – Its status after ten years of operation, in: Proceedings of the Quadrennial Ozone Symposium, edited by: Bojikov, R. D. and Kazuo, S., Sapporo, Japan, 2–8 July 2000, 137–138, 2000.

Manney, G. L., Zurek, R. W., O'Neill, A., and Swinbank, R.: On the motion of air through the stratospheric polar vortex, J. Atmos. Sci., 51, 2973–2994, 1994.

Manney, G. L., Krüger, K., Sabutis, J. L., Sena, S. A., and Pawson, S.: The remarkable 2003–2004 winter and other recent warm winters in the Arctic stratosphere since the late 1990s, J. Geophys. Res., 110, D04107, doi:10.1029/2004JD005367, 2005.

Manney, G. L., Daffer, W. H., Strawbridge, K. B., et al.: The High Arctic in extreme winters: vortex, temperature, and MLS and ACE-FTS trace gas evolution, Atmos. Phys. Chem. Discuss., 7, 10 235–10 285, 2007a.

Manney, G. L., Daffer, W. H., Zawodny, J. M., et al.: Solar occultation satellite data and derived meteorological products: Sampling issues and comparisons with Aura MLS, J. Geophys. Rev., 112, D24S50, doi:10.1029/2007JD008709, 2007b.

McElroy, C. T.: A spectroradiometer for the measurement of direct and scattered solar irradiance from on-board the NASA ER-2 high-altitude research aircraft, Geophys. Res. Lett., 22, 1361–1364, 1995.

McElroy, C. T., Nowlan, C. R., Drummond, J. R., et al.: The ACE-MAESTRO instrument on SCISAT: description, performance, and preliminary results, Appl. Optics, 46, 4341–4356, 2007.

McLinden, C. A., Olsen, S. C., Hannegan, B., Wild, O., Prather, M. J., and Sundet, J.: Stratospheric ozone in 3-D models: A simple chemistry and the cross-tropopause flux, J. Geophys. Res., 105, D11, 14 653–14 665, 2000.

McLinden, C. A., McConnell, J. C., Griffioen, E., and McElroy, C. T.: A vector radiative-transfer model for the Odin/OSIRIS project, Can. J. Phys., 80, 375–393, 2002.

Platt, U.: Differential optical absorption spectroscopy (DOAS), in Air monitoring by spectroscopic techniques, edited by: M. W. Sigrist, 27–84, John Wiley, Hoboken, NJ, 1994.

Pommereau, J. P. and Goutail, F.: O_3 and NO_2 ground-based measurements by visible spectrometry during Arctic winter and spring 1988, Geophys. Res. Lett., 15, 891–894, 1988.

Prather, M. J.: Catastrophic loss of stratospheric ozone in dense volcanic clouds, J. Geophys. Res., 97, 10 187–10 191, 1997.

Randall, C. E., Lumpe, J. D., Bevilacqua, R. M., Hoppel, K. W., Shettle, E. P., Rusch, D. W., Gordley, L. L., Kreher, K., Pfeilsticker, K., Boesch, H., Toon, G., Goutail, F., and Pommereau, J.- P.: Validation of POAM III NO_2 measurements, J. Geophys. Res., 107(D20), doi:10.1029/2001JD001520, 2002.

Roscoe, H. K., Johnstone, P. V., Van Roozendael, M., et al.: Slant column measurements of O_3 and NO_2 during the NDSC intercomparison of zenith-sky UV-visible spectrometers in June 1996, J. Atmosp. Chem., 32, 281–314, 1999.

Rothman, L. S., Jacquemart, D., Barbe, A., et al.: The HITRAN molecular spectroscopic database: edition of 2000 including updates through 2001, J. Quant. Spectrosc. Radiat. Transfer, 82, 5–44, 2003.

Sarkissian, A., Vaughan, G., Roscoe, H. K., Martlett, L. M., O'Connor, F. M., Drew, D. G., Hughes, P. A., and Moore, D. M.: Accuracy of measurements of total ozone by a SAOZ ground-based zenith sky visible spectrometer, J. Geophys. Res., 102(D1), 1379–1390, 1997.

Solomon, S., Schmeltekopf, A. L., and Sanders, R. W.: On the interpretation of zenith sky absorption measurements, J. Geophys. Res., 92, 8311–8319, 1987.

Tarasick, D. W., Filotev, V. E., Wardle, D. I., Kerr, J. B., and Davies, J.: Changes in the vertical distribution of ozone over Canada from ozonesondes: 1980–2001, J. Geophys. Res., 100, D02304, doi:10.1029/2004JD004643, 2005.

Vandaele, A. C., Hermans, C., Simon, P. C., Carleer, M., Colin, R., Fally, S., Mérienne, M. -F., Jenouvrier, A., and Coquart, B.: Measurements of the NO_2 absorption cross-section from 42 000 cm^{-1} to 10 000 cm^{-1} (238–1000 nm) at 220 K and 294 K, J. Quant. Spectrosc. Radiat. Transfer, 59, 171–184, 1998.

Vandaele, A. C., Fayt, C., Hendrick, F. et al.: An intercomparison campaign of ground-based UV-visible measurements of NO_2, BrO, and OClO slant columns: Methods of analysis and results for NO_2, J. Geophys. Res., 110, D08305, doi:10.1029/2004JD005423, 2005.

York, D., Evensen, N. M., López Martínez, M., and De Basabe Delgado, J.: Unified equations for the slope, intercept, and standard errors of the best straight line, Am. J. Phys., 72, 367–375, 2003.